Theoretical Microfluidics

MICRO-718

T. Lehnert and M.A.M. Gijs (EPFL-LMIS2)

EPFL - Lausanne
Doctoral Program in Microsystems and Microelectronics (EDMI)

ÉCOLE POLYTECHNIQUE
FÉDÉRALE DE LAUSANNE

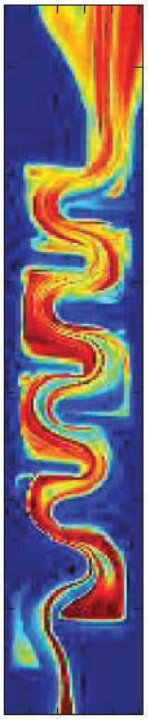

Part II: *M.A.M. Gijs (EPFL-LMIS2)*

Electrohydrodynamics

Basics of microfluidics (MICRO-714) – H. Bruus, M. Gijs, Th. Lehnert

Contents

- Basic equations
- Electrical polarization and dipole moments
- Electrokinetic effects
- The Debye layer near charged surfaces
  - The continuum model of the Debye layer
  - The Debye-Hückel approximation
  - Surface charge and Debye-layer capacitance
  - Impedimetric analysis of liquid solutions
  - Debye-layer screening of a particle

Basic equations

ÉCOLE POLYTECHNIQUE FÉDÉRALE DE LAUSANNE

Including electrical body force in the Navier-Stokes equation:

$$\rho\Big(\partial_t \mathbf{v} + (\mathbf{v}\cdot\boldsymbol{\nabla})\mathbf{v}\Big) = -\boldsymbol{\nabla} p + \eta\nabla^2\mathbf{v} + \rho\,\mathbf{g} + \rho_{\mathrm{el}}\mathbf{E}, \tag{7.1}$$

Maxwell equations in the electrostatic regime:

$$\boldsymbol{\nabla}\times\mathbf{E} = \mathbf{0}, \tag{7.2a}$$

$$\boldsymbol{\nabla}\cdot\mathbf{D} = \boldsymbol{\nabla}\cdot(\epsilon\mathbf{E}) = \rho_{\mathrm{el}}, \tag{7.2b}$$

$$\mathbf{D} = \epsilon_0\mathbf{E} + \mathbf{P} = \epsilon\mathbf{E}, \tag{7.2c}$$

$$\mathbf{J}_{\mathrm{el}} = \sigma_{\mathrm{el}}\mathbf{E}. \tag{7.2d}$$

Following (7.2a): (why?)

$$\mathbf{E} = -\boldsymbol{\nabla}\phi, \tag{7.3a}$$

$$\nabla^2\phi(\mathbf{r}) = -\frac{1}{\epsilon}\,\rho_{\mathrm{el}}(\mathbf{r}). \tag{7.3b}$$

Polarization and dipole moments

ÉCOLE POLYTECHNIQUE FÉDÉRALE DE LAUSANNE

i^{th} component of electrical force on particle with electrical charge density ρ_{el} , occupying region Ω around position $\mathbf{r_0}$:

$$\begin{aligned} F_i &= \int_\Omega \mathrm{d}\mathbf{r}\,\rho_{\mathrm{el}}(\mathbf{r}_0+\mathbf{r})E_i(\mathbf{r}_0+\mathbf{r}) \\ &\approx \int_\Omega \mathrm{d}\mathbf{r}\,\rho_{\mathrm{el}}(\mathbf{r}_0+\mathbf{r})\Big[E_i(\mathbf{r}_0)+r_j\partial_j E_i(\mathbf{r}_0)\Big] \\ &= QE_i(\mathbf{r}_0)+p_j\partial_j E_i(\mathbf{r}_0), \end{aligned} \tag{7.4}$$

with definition of charge (Q) and dipole moment $\mathbf{p}$ of the particle:

$$Q \equiv \int_\Omega \mathrm{d}\mathbf{r}\,\rho_{\mathrm{el}}(\mathbf{r}_0+\mathbf{r}), \tag{7.5a}$$

$$\mathbf{p} \equiv \int_\Omega \mathrm{d}\mathbf{r}\,\rho_{\mathrm{el}}(\mathbf{r}_0+\mathbf{r})\,\mathbf{r}. \tag{7.5b}$$

Point dipole:

$$\rho_{\rm el}(\mathbf{r}_0+\mathbf{r}) = +q\,\delta\big(+\tfrac{1}{2}\mathbf{d}-\mathbf{r}\big) - q\,\delta\big(-\tfrac{1}{2}\mathbf{d}-\mathbf{r}\big),$$

$$\mathbf{p} = q\mathbf{d}. \qquad (7.7)$$

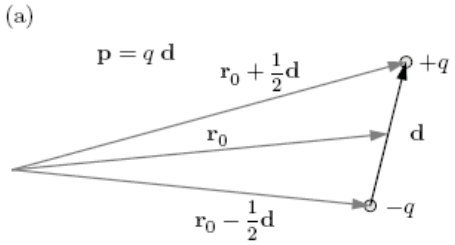

Definition of polarization $\mathbf{P}(\mathbf{r_0})$:

$$\mathbf{P}(\mathbf{r}_0) = \lim_{\mathrm{Vol}(\Omega^*)\to 0}\left[\frac{1}{\mathrm{Vol}(\Omega^*)}\int_{\Omega^*} \mathrm{d}\mathbf{r}\,\rho_{\rm el}(\mathbf{r}_0+\mathbf{r})\,\mathbf{r}\right]. \qquad (7.8)$$

Polarization charge Q_{pol} left in body:

$$Q_{\rm pol} = -\int_{\partial\Omega} \mathrm{d}a\,\mathbf{n}\cdot\left(\frac{q\mathbf{d}}{\mathrm{Vol}(\Omega^*)}\right) = -\int_{\partial\Omega}\mathrm{d}a\,\mathbf{n}\cdot\mathbf{P} = -\int_{\Omega}\mathrm{d}\mathbf{r}\,\boldsymbol{\nabla}\cdot\mathbf{P}. \qquad (7.9)$$

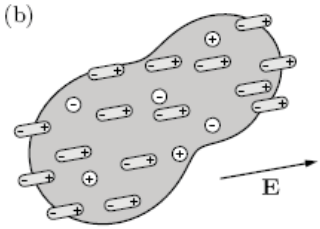

Definition of polarization density ρ_{pol}:

$$\rho_{\rm pol} \equiv -\boldsymbol{\nabla}\cdot\mathbf{P}, \qquad (7.10)$$

$$\rho_{\rm ext} = \rho_{\rm tot} - \rho_{\rm pol} = \epsilon_0\boldsymbol{\nabla}\cdot\mathbf{E} + \boldsymbol{\nabla}\cdot\mathbf{P} = \boldsymbol{\nabla}\cdot\big(\epsilon_0\mathbf{E}+\mathbf{P}\big). \qquad (7.11)$$

$$\mathbf{D} \equiv \epsilon_0\mathbf{E} + \mathbf{P}$$

→ ρ_{el} in (7.2b) should not contain polarization charge.

Electrokinetic effects

- Electrophoresis : the movement of a charged surface (of say dissolved or suspended material) relative to a stationary liquid induced by an applied electric field.
- Electroosmosis : the movement of liquid relative to a stationary charged surface (of say a capillary tube) induced by an applied electric field.
- Sedimentation potential : the electric potential created when charged particles are made to move relative to a stationary liquid.
- Streaming potential : the electric potential created when a liquid is made to move relative to a charged surface.

Electrophoresis

Spherical particle of radius *a* and charge *Ze* in stationary liquid:

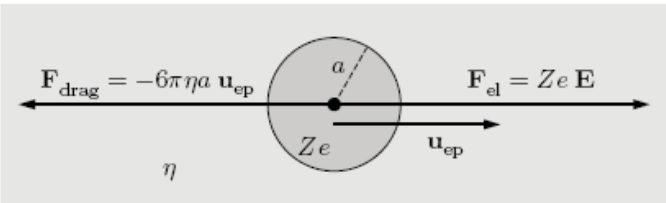

$$\mathbf{F}_{\text{el}} = Ze\mathbf{E}$$

$$\mathbf{F}_{\text{drag}} = -6\pi\eta a\,\mathbf{u}_{\text{ep}}$$

$$\mathbf{F}_{\text{tot}} = \mathbf{F}_{\text{el}} + \mathbf{F}_{\text{drag}} = 0 \quad \Rightarrow \quad \mathbf{u}_{\text{ep}} = \frac{Ze}{6\pi\eta a}\,\mathbf{E} \equiv \mu_{\text{ion}}\,\mathbf{E}. \qquad (7.13)$$

Ionic mobility: $\mu_{\text{ion}} \equiv \dfrac{Ze}{6\pi\eta a}$ $\qquad$ a : hydrated radius ≈ 0.2 nm

ions at $T = 25°C$	H^+	Ag^+	K^+	Li^+	Na^+	Br^-	Cl^-	F^-	I^-	OH^-
mobility μ_{ion} $[10^{-8}\ \text{m}^2\ (\text{V s})^{-1}]$	36.2	6.42	7.62	4.01	5.19	8.09	7.91	5.70	7.96	20.6
diffusivity D_{ion} $[10^{-9}\ \text{m}^2\ \text{s}^{-1}]$	9.31	-	1.96	1.03	1.33	2.08	2.03	1.46	2.05	5.30

Debye layer near charged surfaces

Ions having opposite charge of the solid are attracted, co-ions are repelled. For $z > 0$, the electrolyte is charge-neutral

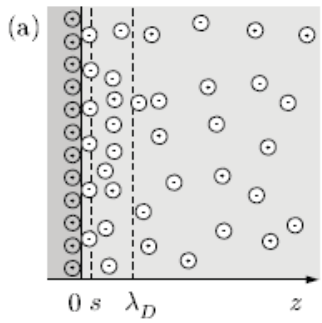

$\mu(\mathbf{r})$: chemical potential for the counter- and co-ion concentrations $c_\pm(\mathbf{r})$, the free energy of the last added ion

$$\mu(\mathbf{r}) = \mu_0 + k_\mathrm{B}T \ln\left(\frac{c_\pm(\mathbf{r})}{c_0}\right) \pm Ze\phi(\mathbf{r}), \qquad (7.18)$$

In thermodynamic equilibrium, the chemical potential is constant

$$\mu(\mathbf{r}) = \text{const} \quad \Rightarrow \quad \nabla\mu(\mathbf{r}) \equiv 0 \quad \Rightarrow \quad k_\mathrm{B}T\nabla \ln\left(\frac{c_\pm(\mathbf{r})}{c_0}\right) = \mp Ze\nabla\phi(\mathbf{r}). \qquad (7.19)$$

Infinitely away from the surface, the two ionic concentrations have the same value c_0 .

Potential at the surface: ζ - potenial .

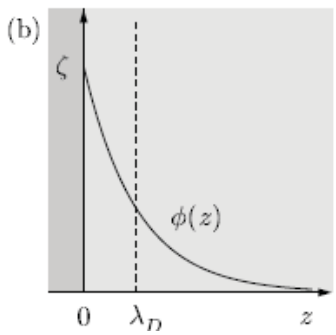

$$c_\pm(\infty) = c_0, \qquad \phi(\infty) = 0, \qquad \phi(\text{surf}) = \zeta.$$

$$c_\pm(\mathbf{r}) = c_0 \exp\left[\mp \frac{Ze}{k_\mathrm{B}T}\phi(\mathbf{r})\right]$$

Solution for the charge density

$$\rho_\mathrm{el}(\mathbf{r}) = Ze\big[c_+(\mathbf{r}) - c_-(\mathbf{r})\big] = -2Zec_0 \sinh\left[\frac{Ze}{k_\mathrm{B}T}\phi(\mathbf{r})\right]$$

leading to the Poisson-Boltzmann equation

$$\nabla^2\phi(\mathbf{r}) = 2\frac{Zec_0}{\epsilon} \sinh\left[\frac{Ze}{k_\mathrm{B}T}\phi(\mathbf{r})\right]$$

Analytical solution for an infinite planar surface, the so-called Gouy-Chapman solution :

$$\phi(z) = \frac{4k_B T}{Ze} \operatorname{arctanh}\left[\tanh\left(\frac{Ze\zeta}{4k_B T}\right) \exp\left(-\frac{z}{\lambda_D}\right)\right]$$

with the so-called Debye length:

$$\lambda_D \equiv \sqrt{\frac{\epsilon k_B T}{2(Ze)^2 c_0}}$$

For c_0 = 1 mM = 1 mol/m^3, $\varepsilon = 78\varepsilon_0$

$$\lambda_D \approx 9.5 \text{ nm}.$$

Debye-Hückel approximation

Debye-Hückel limit : $Ze\zeta \ll k_B T$ → $\sinh(u) \approx u$

$$\nabla^2 \phi(\mathbf{r}) = 2\frac{(Ze)^2 c_0}{\epsilon k_B T}\phi(\mathbf{r}) \equiv \frac{1}{\lambda_D^2}\phi(\mathbf{r}), \qquad (7.28)$$

For an **infinite planar surface**:

$$\partial_z^2 \phi(z) = \frac{1}{\lambda_D^2}\phi(z), \qquad (7.29)$$

Solution:

$$\phi(z) = \zeta \exp\left[-\frac{z}{\lambda_D}\right] \quad (z > 0, \text{ single plate wall})$$

Solution of the Poisson equation (7.3b):

$$\rho_{el}(z) = -\epsilon\partial_z^2\phi(z) = -\frac{\epsilon\zeta}{\lambda_D^2}\exp\left[-\frac{z}{\lambda_D}\right] \quad (z > 0, \text{ single plate wall})$$

Ionic densities found by Taylor expansion of the exponential of $c_{\pm}(\mathbf{r})$

$$c_{\pm}(z) = c_0 \left[1 \mp \frac{Ze\zeta}{k_B T} \exp\left[-\frac{z}{\lambda_D} \right] \right] \quad (z > 0, \text{ single plate wall})$$

$$Ze\zeta \ll k_B T$$

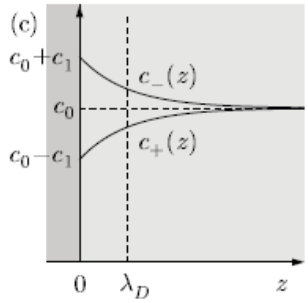

Infinite planar plate channel with surfaces at $z = \pm h/2$ $\phi(\pm h/2) = \zeta$.

$$\phi(z) = \zeta \frac{\cosh\left(\frac{z}{\lambda_D}\right)}{\cosh\left(\frac{h}{2\lambda_D}\right)} \quad \left(-\frac{h}{2} < z < \frac{h}{2}, \text{ parallel-plate channel}\right)$$

$$\rho_{el}(z) = -\frac{\epsilon\zeta}{\lambda_D^2} \frac{\cosh\left(\frac{z}{\lambda_D}\right)}{\cosh\left(\frac{h}{2\lambda_D}\right)} \quad \left(-\frac{h}{2} < z < \frac{h}{2}, \text{ parallel-plate channel}\right)$$

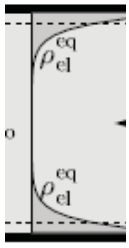

ÉCOLE POLYTECHNIQUE
FÉDÉRALE DE LAUSANNE

Poisson-Boltzmann equation and solution for **circular-shaped channel** with radius a :

$$\left[\partial_r^2 + \frac{1}{r}\partial_r\right]\phi(r) = \frac{1}{\lambda_D^2}\phi(r) \quad (0 < r < a, \text{ circular channel})$$

$$\phi(r) = \zeta \frac{I_0\left(\frac{r}{\lambda_D}\right)}{I_0\left(\frac{a}{\lambda_D}\right)} \quad (0 < r < a, \text{ circular channel})$$

$$\rho_{el}(r) = -\epsilon\nabla^2\phi(r) = -\frac{\epsilon}{\lambda_D^2}\phi(r) = -\frac{\epsilon\zeta}{\lambda_D^2}\frac{I_0\left(\frac{r}{\lambda_D}\right)}{I_0\left(\frac{a}{\lambda_D}\right)} \quad (0 < r < a, \text{ circular channel})$$

Surface charge and Debye-layer capacitance

ÉCOLE POLYTECHNIQUE FÉDÉRALE DE LAUSANNE

Charge per area A contained in the liquid perpendicular to A :

$$q_{\text{liq}} = \int_0^\infty \mathrm{d}z\, \rho_{\text{el}}(z) = \int_0^\infty \mathrm{d}z \left[-\frac{\epsilon\zeta}{\lambda_D^2} \exp\left[-\frac{z}{\lambda_D} \right] \right] = -\frac{\epsilon}{\lambda_D}\zeta. \qquad (7.38)$$

Capacitance per area A of the Debye layer :

$$C_D \equiv \frac{\epsilon}{\lambda_D} \qquad C_D \approx 0.073\ \mathrm{F\ m^{-2}}.$$

Surface charge per area q_{surf} accumulated on the surface.

Total charge in Gauss box : $\mathcal{A} q_{\text{surf}} = \epsilon E \mathcal{A}$. $\nabla \cdot (\epsilon \mathbf{E}) = \rho_{\text{el}}$.

$$q_{\text{surf}} = \epsilon E = -\epsilon \partial_z \phi(0) = \frac{\epsilon}{\lambda_D}\zeta. \qquad (7.41)$$

ÉCOLE POLYTECHNIQUE FÉDÉRALE DE LAUSANNE

Electrolyte between two parallel-plate metallic electrodes:

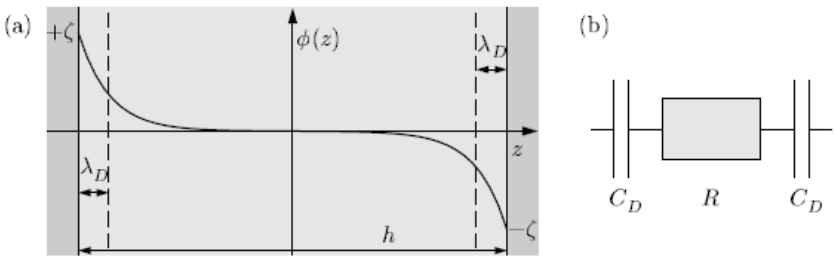

RC time of this system:

$$\tau_{RC} = RC = \left(\frac{h}{\sigma_{\text{el}}\mathcal{A}} \right) \left(\frac{1}{2} \frac{\epsilon}{\lambda_D} \mathcal{A} \right) = \frac{\epsilon}{2\sigma_{\text{el}}} \frac{h}{\lambda_D}. \qquad (7.42)$$

$\lambda_D = 9.6$ nm, $h = 100\ \mu$m, $\epsilon = 78\epsilon_0$, and $\sigma_{\text{el}} = 10^{-3}$ S/m,

$$\boxed{\tau_{RC} = 3.6\ \text{ms}.} \qquad (7.43)$$

For frequencies higher than a few kHz, the Debye layer is not established (effect?).

DNA detection with interdigitated electrodes

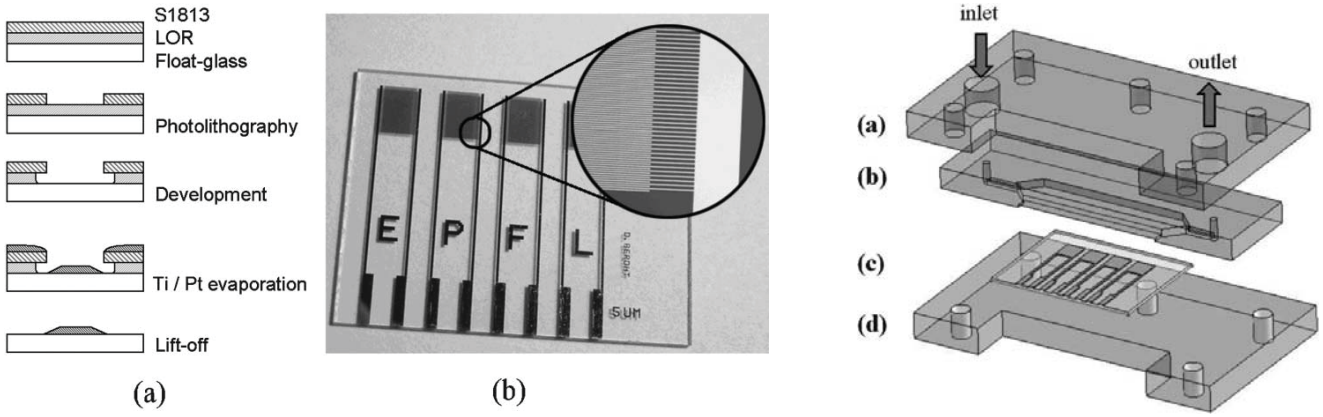

Daniel Berdat, Ana C. Martin Rodrıguez, Fernando Herrera , and Martin A. M. Gijs, Lab Chip 8, 302-308 (2008).

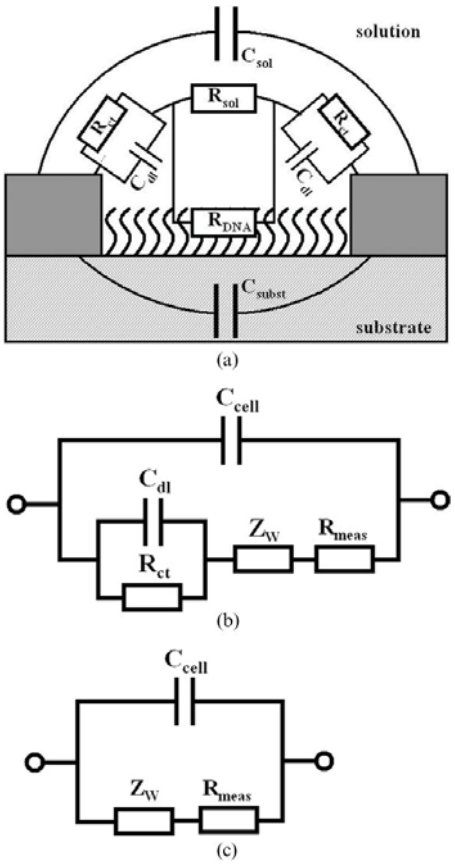

$$R_{meas} = (R_{sol}^{-1} + R_{DNA}^{-1})^{-1}$$

$$R_{sol} = 2\frac{1}{nl}\rho$$

$$C_{cell} = C_{sol} + C_{subst}$$

$$C_{cell} = nl\varepsilon_0\varepsilon_r\frac{1}{2}$$

$$C_{cell} \approx 0.52\ \text{nF} \qquad (n = 400,\ l = 2.9\ \text{mm and}\ \varepsilon_r = 80)$$

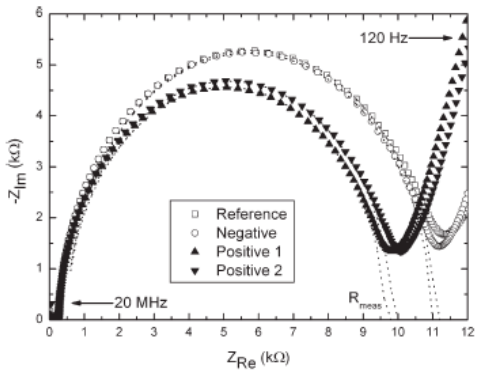

Impedimetry of salt and DNA solutions

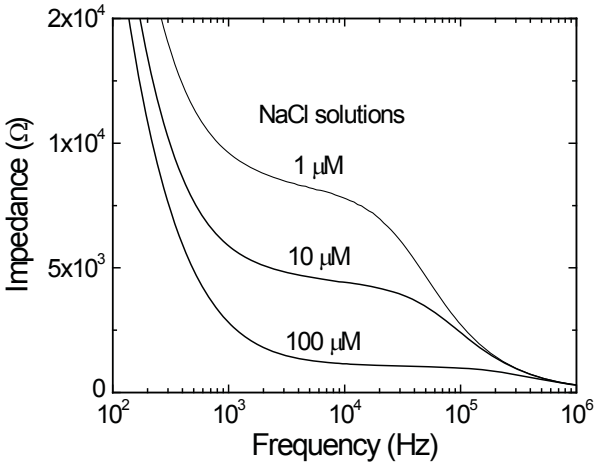

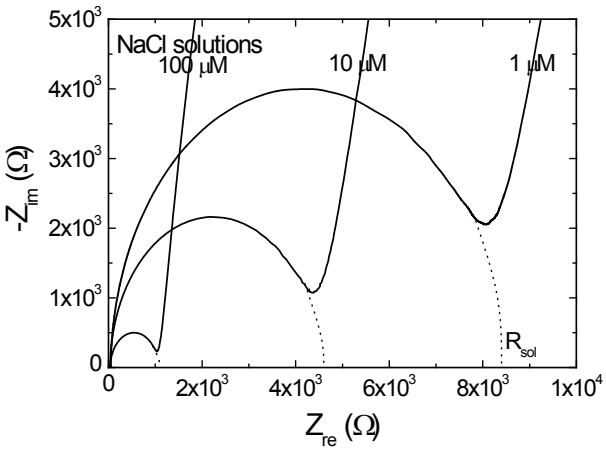

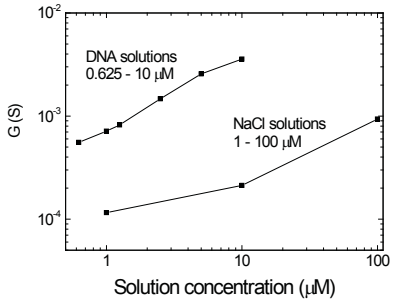

D. Berdat, A. Marin, F. Herrera, and M.A.M. Gijs, Sensors and Actuators B 118, 53-59 (2006).

Debye layer screening of a particle

For spherical particle of radius a : $\phi(a) = \zeta, \qquad \phi(\infty) = 0$

Poisson-Boltzmann equation in the Debye-Hückel approximation:

$$\frac{1}{r^2}\,\partial_r\left(r^2\,\partial_r\phi\right) = \frac{1}{\lambda_D^2}\,\phi \quad \text{(spherical polar coordinates)}$$

substitution: $\psi(r) \equiv r\,\phi(r)$

$$\partial_r^2\psi = \frac{1}{\lambda_D^2}\,\psi \quad \text{(spherical symmetry)}$$

Solution is screened Coulomb potential:

$$\phi(r) = \zeta\,\frac{a}{r}\,\exp\left[\frac{a-r}{\lambda_D}\right] \quad (r > a, \text{ spherical symmetry})$$

ÉCOLE POLYTECHNIQUE
FÉDÉRALE DE LAUSANNE

Electroosmosis

Basics of microfluidics (MICRO-714) – H. Bruus, M. Gijs, Th. Lehnert

ÉCOLE POLYTECHNIQUE
FÉDÉRALE DE LAUSANNE

- Electrohydrodynamic transport theory
- Ideal electro-osmotic flow
- Debye-layer overlap
- Ideal EO flow with backpressure
- The many-channel EO pump
- EO and on-chip electrophoresis with pressure pulse injection

Electrohydrodynamic transport theory

ÉCOLE POLYTECHNIQUE FÉDÉRALE DE LAUSANNE

$\mathbf{J}_\alpha^{el}$: electrical current density of ion α

$\hat{\mathbf{J}}_\alpha^{el} = \mathbf{J}_\alpha^{el}/(Z_\alpha e)$: particle current density of ion α having valence Z_α

$\hat{\mathbf{J}}_\alpha^{conv} = \mathbf{J}_\alpha^{conv}/m_\alpha$: particle current density of ion α due to convection

$\hat{\mathbf{J}}_\alpha^{diff} = \mathbf{J}_\alpha^{diff}/m_\alpha$: particle current density of ion α due to convection

Combining $\mathbf{J}_\alpha \equiv \mathbf{J}_\alpha^{conv} + \mathbf{J}_\alpha^{diff} = \rho_\alpha \mathbf{v} + \mathbf{J}_\alpha^{diff} = c_\alpha \rho \mathbf{v} + \mathbf{J}_\alpha^{diff}$.

and $\mathbf{J}_{el} = \sigma_{el}\mathbf{E}$ gives :

$$\tilde{\mathbf{J}}_\alpha \equiv \tilde{\mathbf{J}}_\alpha^{conv} + \tilde{\mathbf{J}}_\alpha^{diff} + \tilde{\mathbf{J}}_\alpha^{el} = c_\alpha \mathbf{v} - D_\alpha \nabla c_\alpha - \frac{\sigma_\alpha^{el}}{Z_\alpha e}\nabla\phi, \qquad (8.1)$$

Ideal EO flow

ÉCOLE POLYTECHNIQUE FÉDÉRALE DE LAUSANNE

Applying an electrical field $\mathbf{E}_{ext} = -\nabla\Phi_{ext}$ over a channel exerts a body force $\rho_{el}^{eq}\mathbf{E}_{ext}$ on the Debye layer

The Navier-Stokes equation for analyzing EO flow becomes:

$$\rho\left(\partial_t \mathbf{v} + (\mathbf{v}\cdot\nabla)\mathbf{v}\right) = -\nabla p_{ext} + \eta\nabla^2\mathbf{v} - \rho_{el}^{eq}\nabla\phi_{ext}$$

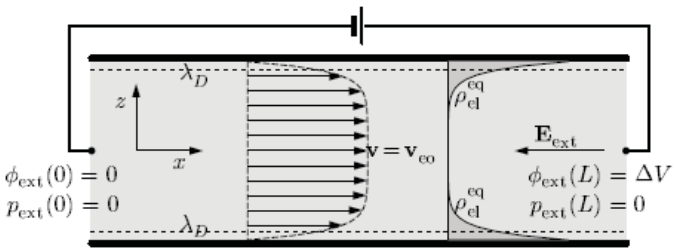

Figure 8.1: The velocity profile $\mathbf{v}$ (dashed line and arrows) and the negative Debye layer charge density profile ρ_{el}^{eq} (dark gray and full line) in an ideal electroosmotic (EO) flow inside a cylindrical channel of radius a and positively charged walls (thick horizontal lines). The EO flow is induced by the external potential difference $\Delta\phi_{ext} = \Delta V$ resulting in the homogeneous electric field $\mathbf{E}_{ext}$. Note how the velocity profile reaches the constant value v_{eo} at a distance of a few times the Debye length λ_D from the walls. No pressure drop is present along the channel in this ideal case.

EOF in parallel plate channel

ÉCOLE POLYTECHNIQUE FÉDÉRALE DE LAUSANNE

Two positively charged walls at z=-h/2 and z=h/2

$$\nabla\phi_{\text{ext}}(\mathbf{r}) = -\mathbf{E} = E\,\mathbf{e}_x, \tag{8.5a}$$
$$\nabla p_{\text{ext}}(\mathbf{r}) = \mathbf{0}, \tag{8.5b}$$
$$\mathbf{v}(\mathbf{r}) = v_x(z)\,\mathbf{e}_x, \tag{8.5c}$$

$$0 = \eta\partial_z^2\, v_x(z) + \left[\epsilon\partial_z^2\,\phi_{\text{eq}}(z)\right] E. \tag{8.6}$$

$$\partial_z^2\left[v_x(z) + \frac{\epsilon E}{\eta}\,\phi_{\text{eq}}(z)\right] = 0. \tag{8.7}$$

$$v_x\left(\pm\frac{h}{2}\right) = 0, \tag{8.8}$$

$$v_x(z) = \left[\zeta - \phi_{\text{eq}}(z)\right]\frac{\epsilon E}{\eta}. \tag{8.9}$$

ÉCOLE POLYTECHNIQUE FÉDÉRALE DE LAUSANNE

Putting in the two-wall potential in the Debye-Hückel limit:

$$v_x(z) = \left[1 - \frac{\cosh\left(\frac{z}{\lambda_D}\right)}{\cosh\left(\frac{h}{2\lambda_D}\right)}\right] v_{\text{eo}}, \tag{8.10}$$

$$v_{\text{eo}} \equiv \frac{\epsilon\zeta}{\eta}\,E. \tag{8.11}$$

Definition of the electroosmotic mobility:

$$\mu_{\text{eo}} \equiv \frac{v_{\text{eo}}}{E} = \frac{\epsilon\zeta}{\eta}. \tag{8.12}$$

$$\zeta \approx 100\ \text{mV}, \qquad \mu_{\text{eo}} \approx 7\times10^{-8}\ \text{m}^2\,(\text{Vs})^{-1}, \qquad v_{\text{eo}} \approx 1\ \text{mm}\,\text{s}^{-1}. \tag{8.13}$$

Note that $\zeta/k_BT \approx 4$ (not Debye-Hückel limit!).

For ideal EO flow:

$$\mathbf{v}(\mathbf{r}) \approx v_{\text{eo}}\, \mathbf{e}_x = -\mu_{\text{eo}}\, \mathbf{E}, \quad \text{for } \lambda_D \ll \frac{1}{2}\, h. \tag{8.14}$$

The free EO flow rate Q_{eo} becomes:

$$Q_{\text{eo}} = \int_{-h/2}^{h/2} \mathrm{d}y \int_0^w \mathrm{d}z\; v_x(y,z) = v_{\text{eo}}\, wh, \quad \text{for } \lambda_D \ll \frac{1}{2}\, h. \tag{8.15}$$

For a cylindrical channel with radius a :

$$\partial_r v_x(0) = 0, \qquad v_x(a) = 0. \tag{8.16}$$

$$v_x(r) = \left[1 - \frac{I_0\left(\frac{r}{\lambda_D}\right)}{I_0\left(\frac{a}{\lambda_D}\right)}\right] v_{\text{eo}}. \tag{8.17}$$

$$Q_{\text{eo}} = \int_0^{2\pi} \mathrm{d}\theta \int_0^a \mathrm{d}r\; r v_x(r,\theta) = v_{\text{eo}}\, \pi a^2, \quad \text{for } \lambda_D \ll a. \tag{8.18}$$

Debye-layer overlap

Suppose λ_D (9.6 nm) becomes of order of the channel radius a, the modified Bessel function can be Taylor-expanded in a/λ_D , giving:

$$v_x(r) \approx \frac{a^2}{4\lambda_D^2}\left[1 - \frac{r^2}{a^2}\right] v_{\text{eo}} + \mathcal{O}\Big((a/\lambda_D)^2\Big). \tag{8.19}$$

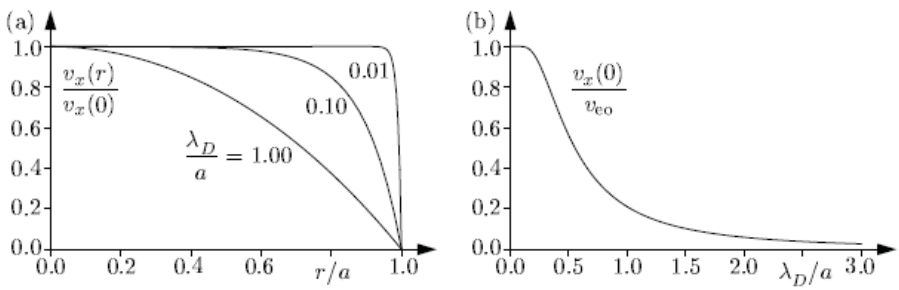

Figure 8.2: (a) The normalized EO flow profile $v_x(r)/v_x(0)$ for a cylindrical channel of radius a with three different values of the Debye length: nearly constant ($\lambda_D/a = 0.01a$), rounded ($\lambda_D/a = 0.1$), and parabolic ($\lambda_D/a = 1$). (b) The maximal velocity in the channel, $v_x(0)$ in units of v_{eo} as a function of λ_D/a. Note that $v_x(0)/v_{\text{eo}} \approx 1$ for $\lambda_D/a < 0.1$ while $v_x(0)/v_{\text{eo}} \approx a^2/(4\lambda_D^2)$ for $\lambda_D/a \gg 1$.

‘Nanofluidics’

Will fluidic electronics take off?

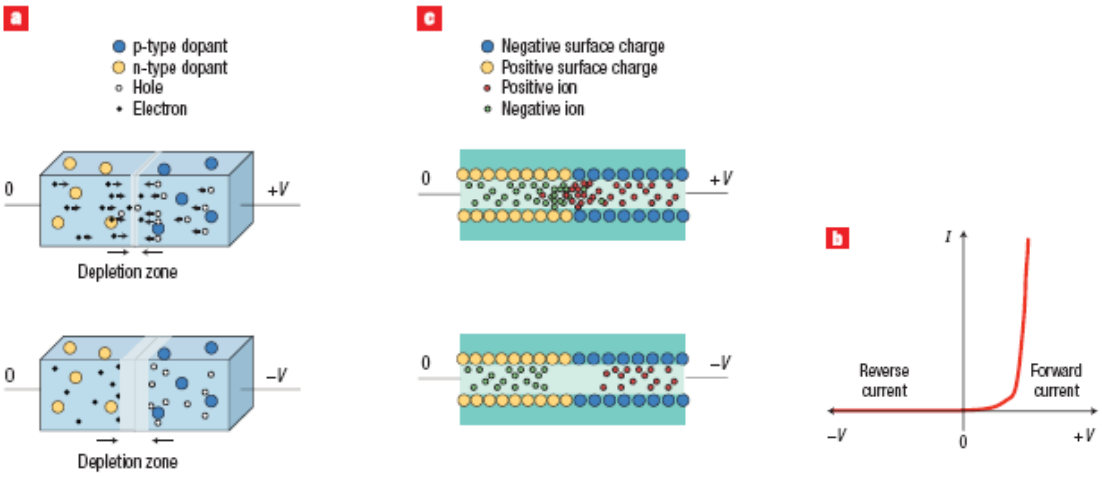

Figure 1 Similarity between nanofluidic and semiconductor diodes. **a**, Operation of a typical semiconductor diode. Fixed impurity atoms (dopants) in the semiconductor contribute mobile holes (p-type, right side) and electrons (n-type, left side). The small black arrows indicate that negative electrons move to the p-type side, whereas positive holes move to the n-type side, until the build up of charge at the interface prevents further charge flow. A positive voltage, *V*, (top diode) makes it easier for current to flow, whereas a negative voltage (bottom diode), makes it more difficult. **b**, As a result, the current–voltage (*I*–*V*) curve is very asymmetric. **c**, In a nanofluidic diode the surface charge on the inner walls of the nanochannel determines which side of the diode is ‘n-type’ and which is ‘p-type’, and the charge carriers are positive and negative ions in the solution. These devices also exhibit a current–voltage curve like the one in (**b**).

M.A.M. Gijs, Nature Nanotechnology 2, 268-270 (2007).

Ideal EO flow with backpressure

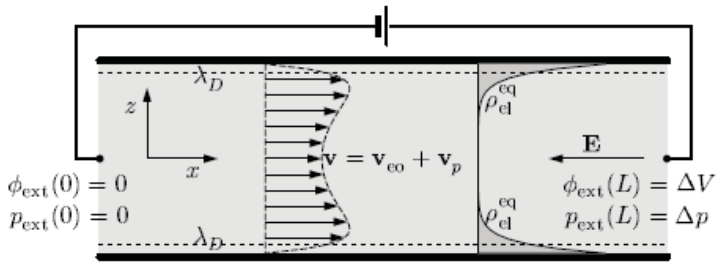

Figure 8.3: The velocity profile $\mathbf{v}$ (dashed line and arrows) and the negative Debye layer charge density profile ρ_{el}^{eq} (dark gray and full line) in an ideal electroosmotic (EO) flow with back-pressure $\Delta p_{ext} = \Delta p$ inside a cylindrical channel of radius a with positively charged walls (thick horizontal lines). The EO flow is induced by the external potential difference $\Delta\phi_{ext} = \Delta V$. Note how the flat EO flow profile $\mathbf{v}_{eo}$ from Fig. 8.1 now has a parabolic dent from the superimposed back-pressure driven Poiseuille flow profile $\mathbf{v}_p$.

$$\phi_{ext}(x=0) = 0 \qquad \phi_{ext}(x=L) = \Delta V \qquad -\nabla\phi_{ext} = \mathbf{E} = -\frac{\Delta V}{L}\,\mathbf{e}_x \tag{8.20a}$$

$$p_{ext}(x=0) = 0 \qquad p_{ext}(x=L) = \Delta p \qquad -\nabla p_{ext} = -\frac{\Delta p}{L}\,\mathbf{e}_x \tag{8.20b}$$

The Navier-Stokes equation becomes, with $\mathbf{v}(\mathbf{r}) = v_x(r)\mathbf{e}_x$:

$$0 = \eta\nabla^2 v_x(r) + \left[\epsilon\nabla^2\phi_{eq}(r)\right]\frac{\Delta V}{L} - \frac{\Delta p}{L}, \tag{8.21}$$

$$v_x(a) = 0, \qquad \partial_r v_x(0) = 0. \tag{8.22}$$

Solution is superposition of EO flow $v_{x,eo}(r)$ and a standard Poiseuille flow $v_{x,p}(r)$ with opposite sign for Δ_p:

$$v_x(r) = v_{x,p}(r) + v_{x,\mathrm{eo}}(r) \tag{8.23a}$$

$$0 = \eta\nabla^2 v_{x,\mathrm{eo}}(r) - \rho_{\mathrm{el}}^{\mathrm{ext}}(r)\frac{\Delta V}{L}, \qquad v_{x,\mathrm{eo}}(a) = 0, \qquad \partial_r v_{x,\mathrm{eo}}(0) = 0, \tag{8.23b}$$

$$0 = \eta\nabla^2 v_{x,p}(r) - \frac{\Delta p}{L}, \qquad v_{x,p}(a) = 0, \qquad \partial_r v_{x,p}(0) = 0. \tag{8.23c}$$

$$v_x(r) = \left[1 - \frac{I_0\left(\frac{r}{\lambda_D}\right)}{I_0\left(\frac{a}{\lambda_D}\right)}\right]\frac{\epsilon\zeta}{\eta}\frac{\Delta V}{L} - \left[a^2 - r^2\right]\frac{1}{4\eta}\frac{\Delta p}{L}. \tag{8.24}$$

Superposition works, because the term $(\mathbf{v}\cdot\nabla)\mathbf{v}$ in the Navier-Stokes equation dropped out due to symmetry reasons.

In the limit $\lambda_D/a << 1$, the flow rate becomes:

$$Q = Q_{\mathrm{eo}} + Q_p = \pi a^2 v_{\mathrm{eo}} - \frac{1}{R_{\mathrm{hyd}}}\Delta p = \frac{\pi a^2 \epsilon\zeta}{\eta L}\Delta V - \frac{\pi a^4}{8\eta L}\Delta p. \tag{8.25}$$

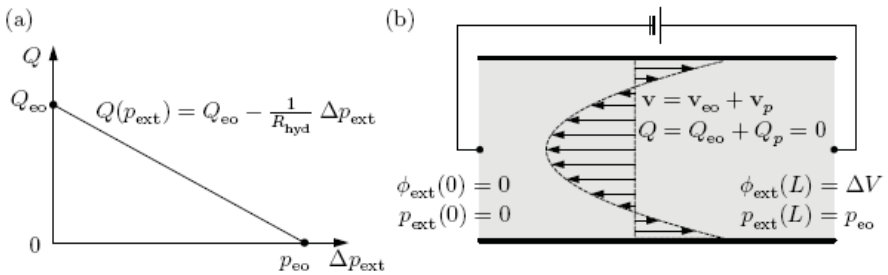

Figure 8.4: (a) The flow rate-pressure characteristic Q–p for an ideal EO flow with back-pressure Δp_{ext}. (b) The flow profile $\mathbf{v}$ in a cylindrical microchannel at maximal back-pressure, the electroosmotic pressure p_{eo}, where the net flow rate is zero, $Q = 0$.

$$Q_{\mathrm{eo}} \equiv \frac{\pi a^2 \epsilon\zeta}{\eta L}\Delta V \qquad \text{at free flow } (Q,p) = (Q_{\mathrm{eo}}, 0), \tag{8.26a}$$

$$p_{\mathrm{eo}} \equiv \frac{Q_{\mathrm{eo}}}{R_{\mathrm{hyd}}} = \frac{8\epsilon\zeta}{a^2}\Delta V \qquad \text{at zero flow } (Q,p) = (0, p_{\mathrm{eo}}). \tag{8.26b}$$

Typical values for Q_{eo} and p_{eo} are found by using $\zeta = 0.1$ V, $a = 10\ \mu$m, $L = 100\ \mu$m, $\eta = 1$ mPa and $\epsilon = 78\epsilon_0$,

$$\frac{Q_{eo}}{\Delta V} = 0.21\ \text{nL s}^{-1}\ \text{V}^{-1}, \tag{8.27a}$$

$$\frac{p_{eo}}{\Delta V} = 5.52\ \text{Pa V}^{-1}. \tag{8.27b}$$

For N channels in parallel, a much higher flow rate can be obtained for the same (low) pressure → EO micropump

$$Q_{eo,N} = NQ_{eo} = N\frac{\pi a^2 \epsilon \zeta}{\eta L}\Delta V \quad \text{at free flow } (Q,p) = (Q_{eo,N}, 0), \tag{8.28a}$$

$$p_{eo,N} = p_{eo} = \frac{8\epsilon\zeta}{a^2}\Delta V \quad \text{at zero flow } (Q,p) = (0, p_{eo,N}). \tag{8.28b}$$

ÉCOLE POLYTECHNIQUE
FÉDÉRALE DE LAUSANNE

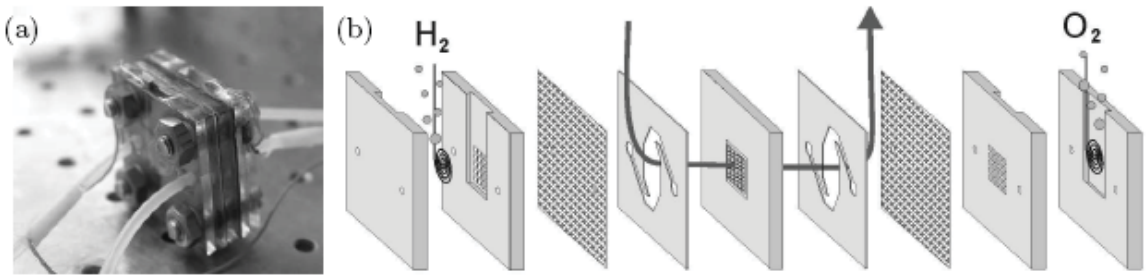

Figure 8.5: (a) A frit-based EO micropump designed and built in the group of Bruus at MIC. For $\Delta V = 30$ V, the pump has $Q_{eo} \approx 0.8\ \mu$L/s and $p_{eo} \approx 4$ kPa, and it can run steadily for hours. (b) The pump consists of layers of polymer sheets micromachined using the laser ablation technique described in Fig. 2.4. The glass frit (gray hatched square) is situated in the central layer. The platinum electrodes (spirals), where gas bubbles are generated by electrolysis, are separated from the liquid flow (the arrow) by anion exchange membranes (white and gray hatched layers), which only allow the passage of OH^- ions.

Brask, Kutter and Bruus (2007).

EOF and on-chip electrophoresis

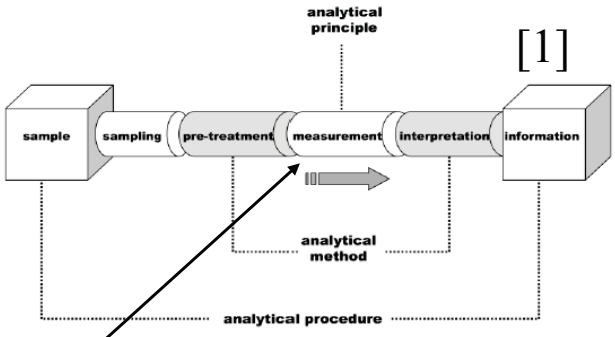

Capillary electrophoresis on-chip

(i) Injection

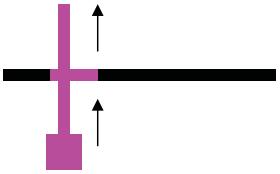

(ii) Separation

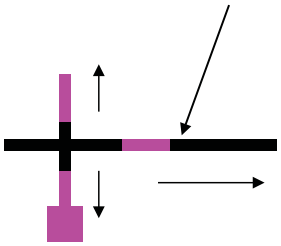

De Mello J. and Beard N., Lab chip, 2003, 11N-19N

Pinched electrokinetic injection (EKI):

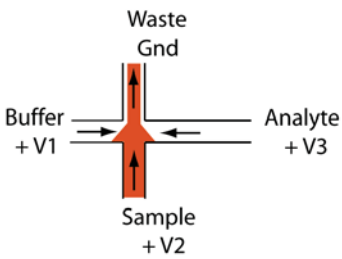

Injection

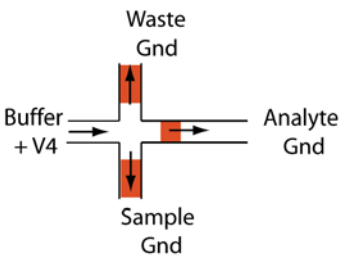

Separation

☺ • Simple technique

☹ • High-voltage switching

☹ • Low analysis frequency

Gated-flow EKI injection using EO flow

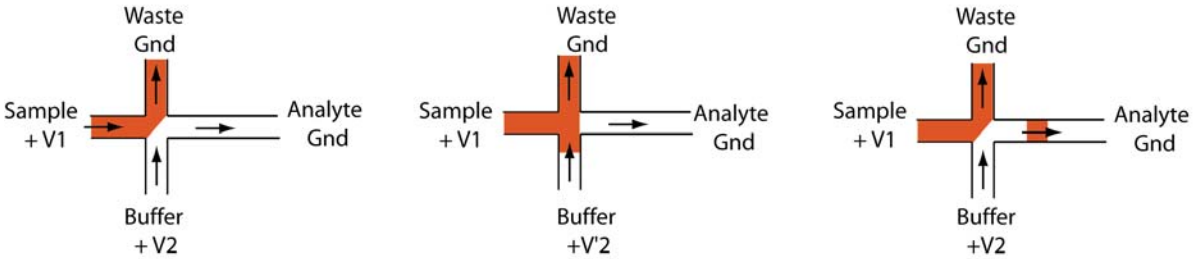

☺ Continuous flow

☺ High analysis frequency

☹ High-voltage switching

☹ Sample composition ≠ analysed plug

Bias: the injected plug does not represent the sample composition

2 compounds with different electrokinetic mobilities

A — $V1$

B — $V2 = 2 \times V$

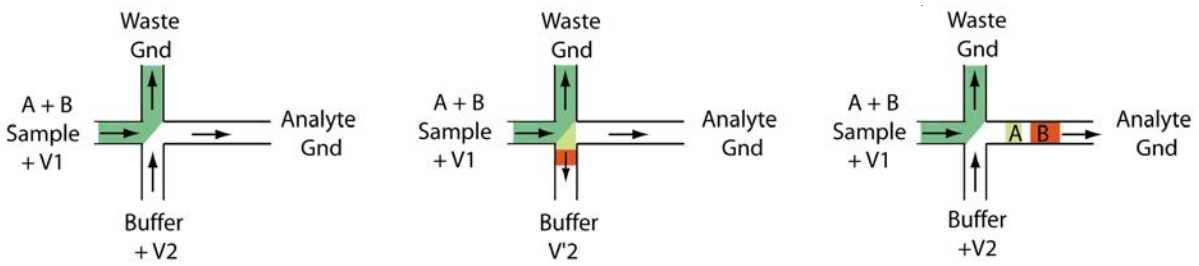

Alarie, J. P.; Jacobson, S. C.; Ramsey, J. M. Electrophoresis 2001, 22, 312-317.
Slentz, B. E.; Penner, N. A.; Regnier, F. Analytical Chemistry 2002, 74, 4835-4840.

Pressure-pulse injection

Integration of an extra pressure reservoir *after* or *before* the channel cross section.

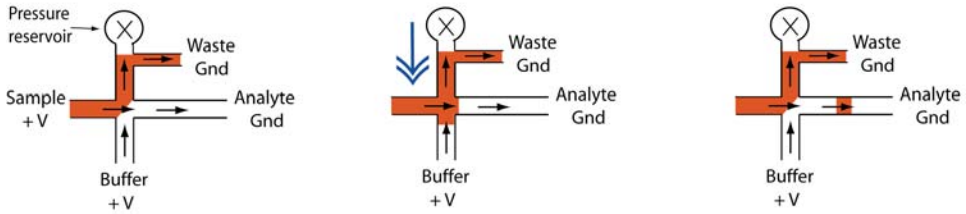

Front Gate Pressure Injection

(FGPI)

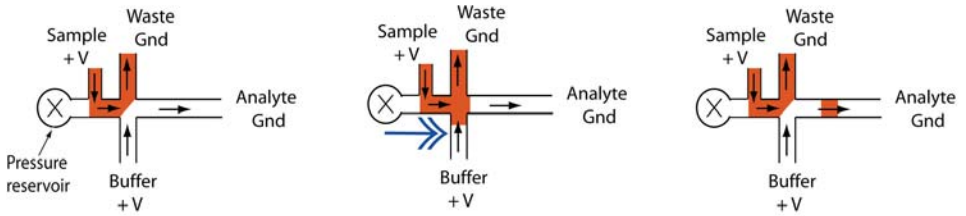

Back Gate Pressure Injection

(BGPI)

☺ Continuous sample flow

☺ No voltage switching: use of one potential

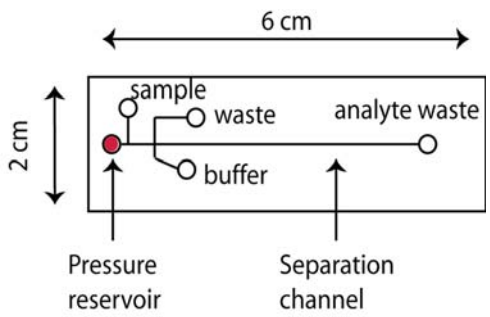

Schematic layout of a BGPI chip

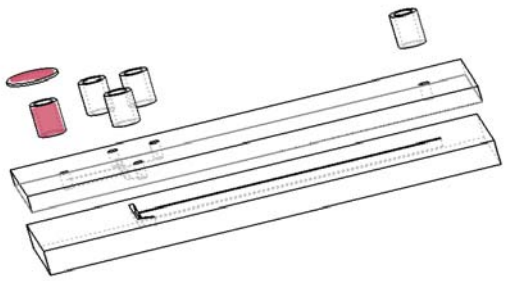

Explosion view of the chip

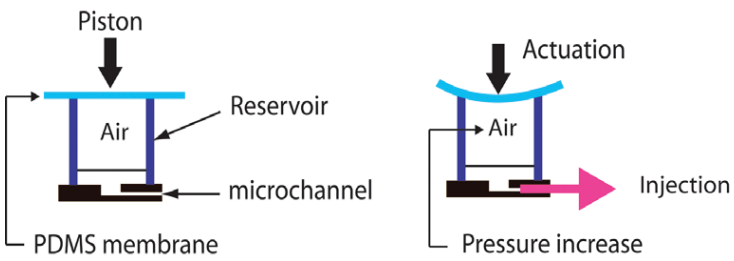

Pressure-pulse injection device

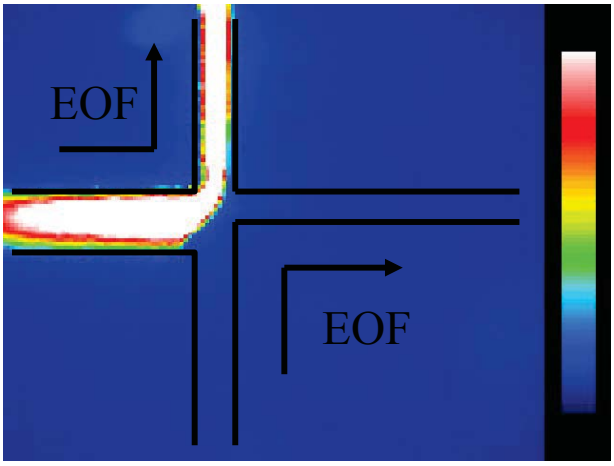

Injection sequence of a 60µM fluorescein plug.

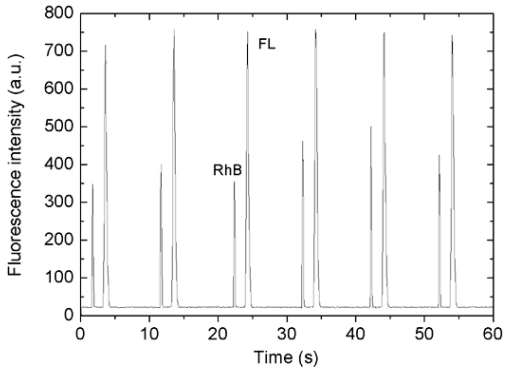

Separation of a mixture of Rhodamine B / Fluorescein

☺ **~ 5% standard deviation**

F. Lacharme and M.A.M. Gijs, Sensors and Actuators B 117(2), 384-390 (2006); F. Lacharme and M.A.M. Gijs, Electrophoresis 27, 2924-2932 (2006).

Dielectrophoresis

Basics of microfluidics (MICRO-714) – H. Bruus, M. Gijs, Th. Lehnert

- Induced polarization and dielectric forces; heuristically
- Point dipole in a dielectric fluid
- Dielectric sphere in a dielectric fluid; induced dipole
- Dielectrophoretic force on a dielectric sphere
- Dielectrophoretic particle trapping in microfluidics
- AC dielectrophoretic force on a dielectric sphere

Dielectrophoresis (DEP)

DEP is the movement of a charge-neutral particle in a dielectric fluid, induced by an inhomogeneous electric field. This driving field can be either DC or AC.

$$\mathbf{P} = \epsilon_0 \chi \, \mathbf{E}, \qquad (9.1)$$

$$\mathbf{p} = \alpha \, \mathbf{E}, \qquad (9.2)$$

Dielectric force $\mathbf{F}_{dip}$ on a dipole moment $\mathbf{p}$ situated in an inhomogeneous electric field (eq. 7.4)

$$\mathbf{F}_{dip} = (\mathbf{p} \cdot \nabla)\mathbf{E}. \qquad (9.3)$$

Polarization and dielectric forces; heuristically

Consider a dielectric sphere with dielectric constant ε_2 placed in a dielectric fluid with dielectric constant ε_1. An inhomogeneous electric field $\mathbf{E}$ is imposed by charging a spherical electrode to the left and a planar electrode to the right.

$$\mathbf{D} = \epsilon_0 \mathbf{E} + \mathbf{P} = \epsilon_0 (1 + \chi)\mathbf{E} = \epsilon \mathbf{E}, \qquad (9.4)$$

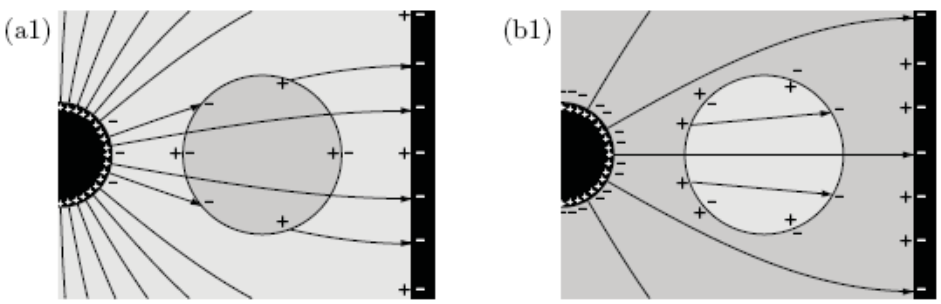

(a1) The particle is more polarizable than the fluid, i.e., $\epsilon_2 > \epsilon_1$. Here the fluid could be vacuum. (b1) The particle is less polarizable than the fluid, i.e., $\epsilon_2 < \epsilon_1$.

Unpaired surface charges induce a dipole moment **p**

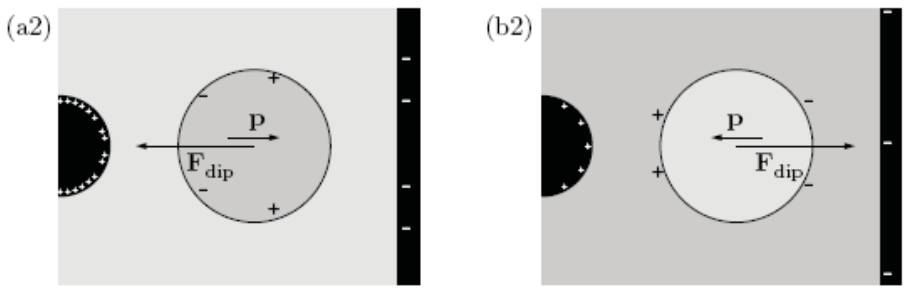

For $\epsilon_1 < \epsilon_2$ the dielectric force pulls the dielectric particle towards the region of strong **E**-field (to the left), while for $\epsilon_1 > \epsilon_2$ the particle is pushed away from this region (towards the right).

Point dipole in a dielectric fluid

Point dipole **p** = q**d** placed in a dielectric fluid with constant ε.

Potential $\phi_{dip}(\mathbf{r})$ from a point dipole, where $d << r$:

$$\mathbf{p} = q\mathbf{d}, \quad \begin{cases} +q \text{ at } +\frac{1}{2}\mathbf{d}, \\ -q \text{ at } -\frac{1}{2}\mathbf{d}. \end{cases} \tag{9.5}$$

$$\phi_{\text{dip}}(\mathbf{r}) = \frac{+q}{4\pi\epsilon}\frac{1}{|\mathbf{r}-\mathbf{d}/2|} + \frac{-q}{4\pi\epsilon}\frac{1}{|\mathbf{r}+\mathbf{d}/2|} \approx \frac{1}{4\pi\epsilon}\frac{\mathbf{p}\cdot\mathbf{r}}{r^3} = \frac{p}{4\pi\epsilon}\frac{\cos\theta}{r^2}, \tag{9.6}$$

θ : angle between dipole **p** and observation vector **r**

Hence, if $\phi_{\text{tot}}(\mathbf{r}) = B\,\frac{\cos\theta}{r^2} + \phi_{\text{rest}}(\mathbf{r}),$ (9.7)

this implies a dipole strength $p = 4\pi\epsilon\, B$ (9.8)

Dielectric sphere in a dielectric fluid; induced dipole

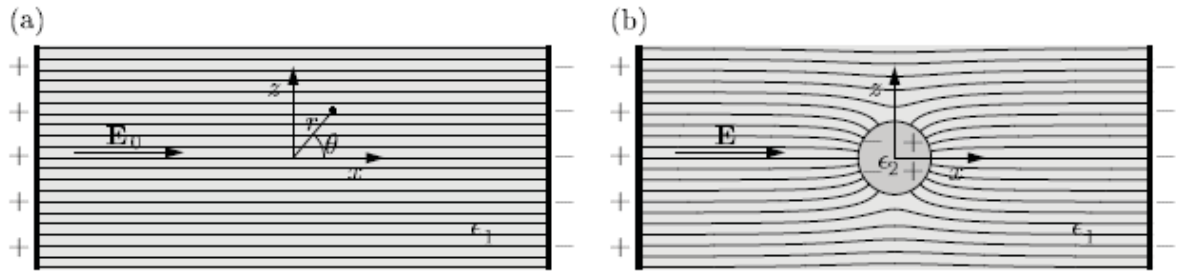

Figure 9.2: (a) A dielectric fluid with a dielectric constant ϵ_1 penetrated by an unperturbed homogeneous electric field $\mathbf{E}_0 = -\nabla\phi_0$, where $\phi_0(r,\theta,\varphi) = -E_0 x = -E_0 r\cos\theta$. (b) A dielectric sphere of radius a and dielectric constant $\epsilon_2 > \epsilon_1$ placed in the dielectric fluid . The electric field polarizes the sphere and a perturbed electric field $\mathbf{E} = -\nabla\phi$ results.

Unperturbed potential ϕ_0 in spherical polar coordinates in the dielectric medium with dielectric constant ε_1 :

$$\phi_0(r,\theta,\varphi) = -E_0\, x(r,\theta,\varphi) = -E_0\, r\cos\theta. \qquad (9.9)$$

Putting a dielectric sphere with radius *a* and dielectric constant ε_2 in the dielectric medium :

$$\phi(r,\theta,\varphi) = \begin{cases} \phi_1(r,\theta), & \text{for } r > a, \\ \phi_2(r,\theta), & \text{for } r < a. \end{cases}, \qquad (9.10)$$

Boundary conditions:

$$\phi_2(0,\theta) \text{ is finite}, \qquad (9.11a)$$
$$\phi_1(a,\theta) = \phi_2(a,\theta), \qquad (9.11b)$$
$$\epsilon_1\partial_r\phi_1(a,\theta) = \epsilon_2\partial_r\phi_2(a,\theta), \qquad (9.11c)$$
$$\phi_1(r,\theta) \underset{r\to\infty}{\longrightarrow} -E_0 r\cos\theta. \qquad (9.11d)$$

(9.11b) : tangential component ($\mathbf{e}_\theta$) of **E** is continuous across surface

(9.11d) : normal component ($\mathbf{e}_r$) of **D**=ε**E** is continuous across surface

$$\nabla \equiv \mathbf{e}_r\partial_r + \mathbf{e}_\theta\frac{1}{r}\,\partial_\theta + \mathbf{e}_\phi\frac{1}{r\sin\theta}\,\partial_\phi. \qquad (A.28)$$

Dielectric media without external charges : $\rho_{el} = 0$

$$\nabla^2 \phi(\mathbf{r}) = 0. \qquad (9.12)$$

No dependence on azimuhal angle ϕ , general solution in terms of Legendre polynomials P_l :

$$\phi(r,\theta) = \sum_{l=0}^{\infty} \left[A_l r^l + B_l r^{-(l+1)} \right] P_l(\cos\theta). \qquad (9.13)$$

Boundary condition (9.11d) → trial solution $P_l(\cos\theta) = \cos\theta$

$$\phi_1(r,\theta) = -E_0 r \cos\theta + B \frac{\cos\theta}{r^2}, \text{ for } r > a, \qquad (9.14a)$$

$$\phi_2(r,\theta) = A r \cos\theta, \text{ for } r < a. \qquad (9.14b)$$

Boundary condition (9.11b) and (9.11c) :

$$-E_0 a + \frac{1}{a^2} B = a\, A, \qquad A = \frac{-3\epsilon_1}{\epsilon_2 + 2\epsilon_1} E_0,$$

$$-E_0 - \frac{2}{a^3} B = \frac{\epsilon_2}{\epsilon_1} A, \qquad B = \frac{\epsilon_2 - \epsilon_1}{\epsilon_2 + 2\epsilon_1} a^3 E_0.$$

Solution for electrical potentials :

$$\phi_1(\mathbf{r}) = -E_0 r \cos\theta + \frac{\epsilon_2 - \epsilon_1}{\epsilon_2 + 2\epsilon_1} a^3 E_0 \frac{\cos\theta}{r^2} = \phi_0(\mathbf{r}) + \phi_{\text{dip}}(\mathbf{r}), \text{ for } r > a, \qquad (9.17a)$$

$$\phi_2(\mathbf{r}) = \frac{-3\epsilon_1}{\epsilon_2 + 2\epsilon_1} E_0 r \cos\theta = \frac{3\epsilon_1}{\epsilon_2 + 2\epsilon_1} \phi_0(\mathbf{r}), \text{ for } r < a. \qquad (9.17b)$$

Dipole moment **p** induced in the sphere:

$$\mathbf{p} = 4\pi\epsilon_1 \frac{\epsilon_2 - \epsilon_1}{\epsilon_2 + 2\epsilon_1} a^3 \mathbf{E}_0. \qquad (9.18)$$

prefactor is the Clausius-Mossotti factor $K(\varepsilon_1, \varepsilon_2)$:

$$K(\epsilon_1, \epsilon_2) \equiv \frac{\epsilon_2 - \epsilon_1}{\epsilon_2 + 2\epsilon_1}. \qquad (9.19)$$

Dielectrophoretic force on a dielectric sphere

ÉCOLE POLYTECHNIQUE FÉDÉRALE DE LAUSANNE

Consider *a* radius of sphere, centered at $\mathbf{r}_0$, much smaller that the distance *l* over which the external electrical field **E** is varying. Taylor expansion of the electrical field $\mathbf{E}_0(\mathbf{r})$ gives :

$$\mathbf{E}_0(\mathbf{r}) \approx \mathbf{E}_0(\mathbf{r}_0) + \left[(\mathbf{r}-\mathbf{r}_0)\cdot\nabla\right]\mathbf{E}_0(\mathbf{r}_0) = \mathbf{E}_0(\mathbf{r}_0) + \mathcal{O}(a/\ell). \qquad (9.20)$$

Generalizing (9.18) :

$$\mathbf{p} \approx a^3 4\pi\epsilon_1 K(\epsilon_1,\epsilon_2)\mathbf{E}_0(\mathbf{r}_0) + a^4\left[\mathbf{f}_1(\epsilon_1,\epsilon_2)\cdot\nabla\right]\mathbf{E}_0(\mathbf{r}_0) = a^3 4\pi\epsilon_1 K(\epsilon_1,\epsilon_2)\mathbf{E}_0(\mathbf{r}_0) + \mathcal{O}(a/\ell). \qquad (9.21)$$

$f_1(\varepsilon_1,\varepsilon_2)$: generalized Clausius-Mossotti function

$$\begin{aligned}\mathbf{F}_{\text{dip}}(\mathbf{r}_0) &= \left[\mathbf{p}(\mathbf{r}_0)\cdot\nabla\right]\mathbf{E}_0(\mathbf{r}_0) + \mathcal{O}(a/\ell)\\ &= 4\pi\epsilon_1\,\frac{\epsilon_2-\epsilon_1}{\epsilon_2+2\epsilon_1}\,a^3\left[\mathbf{E}_0(\mathbf{r}_0)\cdot\nabla\right]\mathbf{E}_0(\mathbf{r}_0) + \mathcal{O}(a/\ell)\\ &= 2\pi\epsilon_1\,\frac{\epsilon_2-\epsilon_1}{\epsilon_2+2\epsilon_1}\,a^3\nabla\left[\mathbf{E}_0(\mathbf{r}_0)^2\right] + \mathcal{O}(a/\ell). \qquad (9.22)\end{aligned}$$

Dielectrophoretic particle trapping

ÉCOLE POLYTECHNIQUE FÉDÉRALE DE LAUSANNE

This kind of dipole force is called a dielectrophoretic force:

$$\mathbf{F}_{\text{DEP}}(\mathbf{r}_0) = 2\pi\epsilon_1\,K(\epsilon_1,\epsilon_2)\,a^3\nabla\left[\mathbf{E}_0(\mathbf{r}_0)^2\right]. \qquad (9.23)$$

A DEP force can trap dielectric particles from a flow if

$$|\mathbf{F}_{\text{DEP}}| > |\mathbf{F}_{\text{drag}}|, \qquad (9.24)$$

Example: rectangular channel with length *L*, width *w* and height *h* (*h*<<*w*). Pressure drop Δp generates flow profile

$$\mathbf{v} = v_x(z)\mathbf{e}_x$$

$$v_x(z) = \frac{\Delta p}{2\eta L}\,(h-z)z = 6\left(1-\frac{z}{h}\right)\frac{z}{h}\,v_0, \qquad (9.25)$$

Inhomogeneous electric field is created by applying potential $\phi=\Delta V$ to spherical metallic electrode of radius r_0 situated at $\mathbf{r}=0$ and potential $\phi=0$ to a ceiling cover plate at $\mathbf{r}=h\mathbf{e}_z$.

Liquid has vanishing conductivity → no Debye screening near electrodes.

Electrical potential constructed by the mirror-image charge method → $\phi(\mathbf{r}) = \frac{r_0}{|\mathbf{r}|}\Delta V - \frac{r_0}{|\mathbf{r} - 2h\mathbf{e}_z|}\Delta V,$ (9.27) $\phi(\mathbf{r} = h\mathbf{e}_z) \equiv 0.$

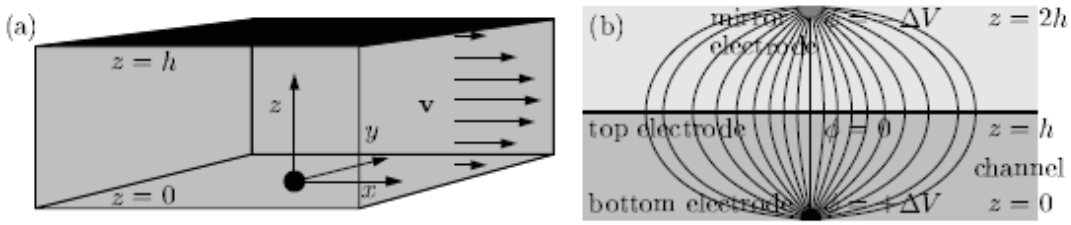

Figure 9.3: (a) An example of DEP trap in a rectangular microfluidic channel of dimensions $L \times w \times h$ to catch dielectric particle suspended in a liquid flow with velocity profile $\mathbf{v}$. An inhomogeneous electric field $\mathbf{E}$ is created by applying a voltage difference ΔV between the (semi-)spherical electrode at the bottom of the microchannel and the planar electrode covering the top. Through the DEP force the bottom electrode will attract the suspended dielectric particles. (b) The electrical field lines calculated by the method of image charges for the potential $\phi(\mathbf{r})$. The spherical bottom electrode at $\mathbf{r} = \mathbf{0}$ has the potential $\phi(\mathbf{0}) = \Delta V$. The planar top electrode of potential $\phi(h\mathbf{e}_z) = 0$ can be realized by placing a mirror electrode with the potential $\phi(2h\mathbf{e}_z) = -\Delta V$ at $\mathbf{r} = 2h\mathbf{e}_z$.

Trapping of particles takes place near the spherical electrode, i.e. $|\mathbf{r}| << h$

$$\mathbf{E}(\mathbf{r}) = -\nabla\phi(\mathbf{r}) \approx \frac{r_0 \Delta V}{r^2}\,\mathbf{e}_r, \text{ for } r_0 < |\mathbf{r}| \ll h. \qquad (9.28)$$

$$\mathbf{F}_{\mathrm{DEP}}(\mathbf{r}) = 2\pi\epsilon_1 \frac{\epsilon_2 - \epsilon_1}{\epsilon_2 + 2\epsilon_1} a^3 \nabla\left[\frac{(\Delta V)^2 r_0^2}{r^4}\right] = -8\pi \frac{\epsilon_2 - \epsilon_1}{\epsilon_2 + 2\epsilon_1} \frac{a^3 r_0^2}{r^5} \epsilon_1 (\Delta V)^2\,\mathbf{e}_r. \qquad (9.29)$$

Maximum DEP force on particle with radius a is achieved at $r = r_{\min} = r_0 + a$. Put $r_0 = \Gamma a$.

$$r_{\min} = (1+\Gamma)a, \quad \Gamma \equiv \frac{r_0}{a}. \qquad (9.30)$$

$$F_{\mathrm{DEP}}^{\max} \equiv |\mathbf{F}_{\mathrm{DEP}}(r_{\min})| = 8\pi \frac{\epsilon_2 - \epsilon_1}{\epsilon_2 + 2\epsilon_1} \frac{\Gamma^2}{(1+\Gamma)^5} \epsilon_1 (\Delta V)^2. \qquad (9.31)$$

Average flow velocity at the position $z = r_0 + a = (1+\Gamma)a$:

$$v_x(r_0+a) = 6\left(1-(1+\Gamma)\frac{a}{h}\right)(1+\Gamma)\frac{a}{h}v_0 \approx 6(1+\Gamma)\frac{a}{h}v_0. \qquad (9.32)$$

$$|\mathbf{F}_{\text{drag}}(r_0+a)| \approx 6\pi\eta\, a\, v_x(r_0+a) = 36\pi(1+\Gamma)\frac{\eta a^2}{h}v_0. \qquad (9.33)$$

Largest average flow velocity v_0^{max} that still allows trapping of particles at the spherical electrode is found form the condition $F_{\text{drag}} = F_{\text{DEP}}^{\text{max}}$, giving

$$v_0^{\max} = \frac{4}{9}\frac{\epsilon_2-\epsilon_1}{\epsilon_2+2\epsilon_1}\frac{\Gamma^2}{(1+\Gamma)^6}\frac{h\epsilon_1(\Delta V)^2}{\eta a^2}. \qquad (9.34)$$

To obtain trapping we need a liquid with a dielectric constant smaller than that of the particle. Let us therefore use the liquid benzene with $\epsilon_1 = 2.28\,\epsilon_0$ and $\eta = 0.65$ mPa s and pyrex glass particles with $\epsilon_2 = 6.0\,\epsilon_0$. The length scales are set to $a = r_0 = 5\,\mu$m and $h = 100\,\mu$m, while the applied voltage drop is $\Delta V = 10$ V. With these parameters we find

$$v_0^{\max} = 3.0 \text{ cm/s}. \qquad (9.35)$$

AC dielectrophoretic force on a dielectric sphere

Advantages of using AC voltage

- ions in the liquid will not change their mean position
- avoids formation of Debye screening layers
- DEP trapping works, even when the liquid and particle have non-zero conductivities, $\sigma_{\text{el},1}$ and $\sigma_{\text{el},2}$.
- Clausius-Mossotti factor depends on the driving frequency ω.

In the following we shall study a simple harmonic time-variation $\exp(-i\omega t)$ (meaning that we must take the real part at the end). In that case the applied potential $\phi(\mathbf{r},t)$ and the associated electrical field $\mathbf{E}(\mathbf{r},t) = -\nabla\phi(\mathbf{r},t)$ have the forms

$$\phi(\mathbf{r},t) \equiv \phi(\mathbf{r})\, e^{-i\omega t}, \qquad (9.36a)$$

$$\mathbf{E}(\mathbf{r},t) \equiv \mathbf{E}(\mathbf{r})\, e^{-i\omega t}. \qquad (9.36b)$$

Intermezzo

ÉCOLE POLYTECHNIQUE FÉDÉRALE DE LAUSANNE

The time average of a product of time-dependent functions

Consider the real physical quantities $A(t)$ and $B(t)$ with harmonic time-variation,

$$A(t) = \mathrm{Re}\left[A_0 e^{-i\omega t}\right], \qquad B(t) = \mathrm{Re}\left[B_0 e^{-i\omega t}\right], \tag{9.48}$$

where A_0 and B_0 are complex amplitudes. Prove that the time-average $\langle A(t)B(t)\rangle$ over one full period τ is given by

$$\langle A(t)B(t)\rangle \equiv \frac{1}{\tau}\int_0^\tau \mathrm{d}t\, A(t)B(t) = \frac{1}{2}\,\mathrm{Re}\left[A_0 B_0^*\right]. \tag{9.49}$$

Hint: rewrite $A(t)B(t)$ using that $\mathrm{Re}\left[Z\right] = \frac{1}{2}\left[Z + Z^*\right]$ for any complex number Z.

ÉCOLE POLYTECHNIQUE FÉDÉRALE DE LAUSANNE

Expression for the DEP force taking AC fields and conductivity into account. Boundary condition for the radial component $E_r(r,\theta) = -\partial_r \phi(a,\theta)$ at the surface of the dielectric sphere :

$$\epsilon_1 E_{r,1}(a,\theta,t) - \epsilon_2 E_{r,2}(a,\theta,t) = q_{\mathrm{surf}}. \tag{9.39}$$

Time-derivative of q_{surf} :

$$\partial_t q_{\mathrm{surf}}(t) = J_{r,1}(a,\theta,t) - J_{r,2}(a,\theta,t) = \sigma_{\mathrm{el},1} E_{r,1}(a,\theta,t) - \sigma_{\mathrm{el},2} E_{r,2}(a,\theta,t). \tag{9.40}$$

Time-derivative of (9.39) and combine with (9.40)

$$\left(\epsilon_1 - i\frac{\sigma_{\mathrm{el},1}}{\omega}\right) E_{r,1}(a,\theta) = \left(\epsilon_2 - i\frac{\sigma_{\mathrm{el},2}}{\omega}\right) E_{r,2}(a,\theta). \tag{9.41}$$

Definition of the complex dielectric function $\varepsilon(\omega)$

$$\epsilon(\omega) \equiv \epsilon - i\frac{\sigma}{\omega}, \tag{9.42}$$

Boundary condition (9.41) with the complex dielectric function looks like boundary condition (9.11c) for the DC case, giving

$$\mathbf{F}_{\mathrm{DEP}}(\mathbf{r}_0,t) = 2\pi\epsilon_1 \frac{\epsilon_2(\omega)-\epsilon_1(\omega)}{\epsilon_2(\omega)+2\epsilon_1(\omega)}\, a^3\nabla\left[\mathbf{E}(\mathbf{r}_0,t)^2\right]. \tag{9.43}$$

To obtain the real time-averaged DEP force $\langle\mathbf{F}_{\mathrm{DEP}}\rangle$ for the complex result Eq. (9.43) we use Eq. (9.38) with $A(t) = K\left[\epsilon_1(\omega),\epsilon_2(\omega)\right]\mathbf{E}(\mathbf{r}_0,t)$ and $B(t) = \mathbf{E}(\mathbf{r}_0,t)$. The result is

$$\langle\mathbf{F}_{\mathrm{DEP}}(\mathbf{r}_0,\omega)\rangle = 2\pi\epsilon_1 \,\mathrm{Re}\left[\frac{\epsilon_2(\omega)-\epsilon_1(\omega)}{\epsilon_2(\omega)+2\epsilon_1(\omega)}\right] a^3\nabla\left[\mathbf{E}_{\mathrm{rms}}(\mathbf{r}_0)^2\right]. \tag{9.44}$$

$$\mathbf{E}_{\mathrm{rms}} = \mathbf{E}/\sqrt{2}.$$

ÉCOLE POLYTECHNIQUE
FÉDÉRALE DE LAUSANNE

Critical frequency ω_c at which the sign of $\langle\mathbf{F}_{\mathrm{DEP}}(\mathbf{r}_0,\omega)\rangle$ changes is found from the condition

$$\mathrm{Re}\left\{\left[\epsilon_2(\omega_c)-\epsilon_1(\omega_c)\right]\left[\epsilon_2(\omega_c)+2\epsilon_1(\omega_c)\right]^*\right\} = 0,$$

$$\omega_c = \sqrt{\frac{(\sigma_{\mathrm{el},1}-\sigma_{\mathrm{el},2})(\sigma_{\mathrm{el},2}+2\sigma_{\mathrm{el},1})}{(\epsilon_2-\epsilon_1)(\epsilon_2+2\epsilon_1)}}. \tag{9.45}$$

Let us calculate a characteristic value for ω_c for a biological cell, consisting mainly of the cytoplasm, in water. We use the following parameters: $\sigma_{\mathrm{el},2} = 0.1$ S/m and $\epsilon_2 = 60.0\epsilon_0$ for the cell, and $\sigma_{\mathrm{el},1} = 0.01$ S/m and $\epsilon_1 = 78.0\epsilon_0$ for water. The value obtained is

$$\omega_c = 1.88\times 10^8 \text{ rad/s}. \tag{9.46}$$

The DEP force can be used to separte living cells from dead cells or cancer cells from normal cells.

ÉCOLE POLYTECHNIQUE
FÉDÉRALE DE LAUSANNE

Magnetophoresis

Basics of microfluidics (MICRO-714) – H. Bruus, M. Gijs, Th. Lehnert

ÉCOLE POLYTECHNIQUE
FÉDÉRALE DE LAUSANNE

- Magnetic and non-magnetic cells
- Magnetic beads
- Magnetostatics
- Magnetic force
- Separation system
- Magnetic lab-on-a-chip for immunoassays

Magnetic cell types

- Red blood cell (RBC), consisting for 97 % of hemoglobin, is magnetic in the de-oxygenized state

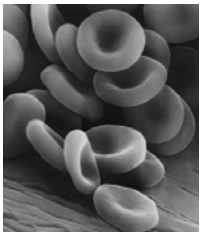

$$\Delta\chi_{oxy} \equiv \chi_{RBC,oxy} - \chi_{water} = -0.19\times10^{-6}$$

$$\Delta\chi_{deoxy} \equiv \chi_{RBC,deoxy} - \chi_{water} = 3.3\times10^{-6}$$

$$\chi_{water} = -9.0\times10^{-6}$$

- Magnetotactic bacterium

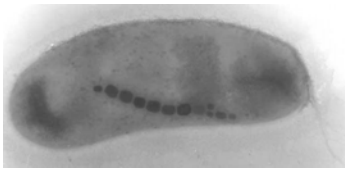

3

Non-magnetic cell types

Cell type	Quantity/microlitre	Fraction of WBC (%)
Red blood cells (RBCs)	5×10^6	
Reticulocytes	$3\text{-}7\times10^4$	
Platelets	$2\text{-}5\times10^5$	
White blood cells (WBCs)	$5\text{-}10\times10^3$	100
Neutrophils	$4\text{-}8\times10^3$	40-65
Monocytes	$2\text{-}8\times10^2$	4-8
Eosinophils	50-300	1-3
Basophils	0-100	0-1
Lymphocytes (total)	1000-4000	20-40
CD4+ T Cell	400-1600	15-20
CD8+ T Cell	200-800	7-10
B Cell	200-800	7-10
Natural Killer Cell	100-500	4-6

4

Cluster of differentiation (CD)

- Protocol for precise identification of cell surface molecules present on WBCs and other cell types
- A combination of CD markers is used to classify cells
- Cell populations are defined using a + or a - symbol to indicate whether a certain cell fraction expresses or lacks a CD molecule.

Cell type	CD markers
Stem cells	CD34+, CD31-
All leukocytes	CD45+
Monocytes	CD45+, CD14+
T cells	CD45+, CD3+
B cells	CD45+, CD19+, or CD45+, CD20+
Natural Killer cells	CD16+, CD56+, CD3-

Magnetic beads

If cells or molecules can be *selectively* labeled with magnetic particles (beads), they can be *selectively* manipulated with magnetic field gradients.

In DEP, the *non-selective* strong dielectric response of both target and auxiliary particles can compromise the functionality of a DEP device.

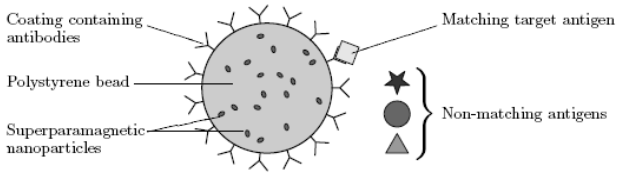

Figure 10.1: A typical polystyrene microbead used for magnetic separation in lab-on-a-chip systems. The bead has a radius of about 1 μm contains inclusions in the form of paramagnetic nanoparticles. The surface is coated with a specific antibody chosen to capture a given target antigen (white square) and not to interact with any other antigens (triangle, pentagram, and circle).

Cell labeling with magnetic beads

- Rare cells in blood, like bacteria, tumor cells or fetal cells in maternal blood occur in concentrations of ten to a hundred cells per milliliter
- Magnetic beads can play a prominent role in purification, if they specifically bind to CD markers on the cell surface

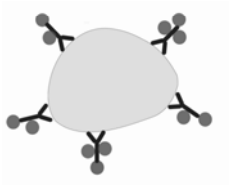

- Also intracellular uptake of superparamagnetic iron oxide nanoparticles is possible

7

Magnetic beads

- Particles containing magnetic material
- Size: 50 nm – 30 μm
- Mostly superparamagnetic
- Become magnetized and are transportable in an external magnetic field
- Coated with polymer or glass surface → coupling of selected molecules
- Essential for high-sensitivity diagnostics

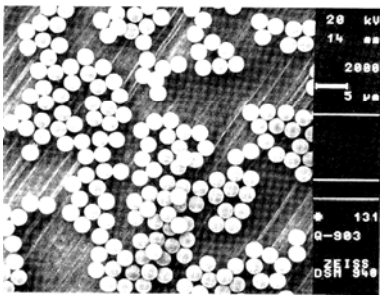

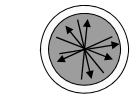

H=0 → <**M(t)**> = 0

H≠0 → <**M(t)**> ≠ 0

8

Superparamagnetic versus ferromagnetic beads

Depends on size and magnetic content (Fe_3O_4)

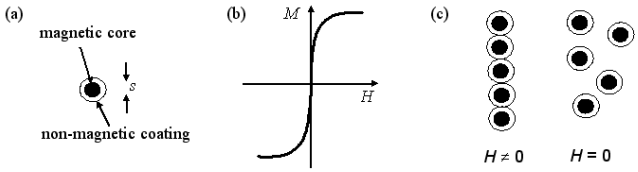

superparamagnetic

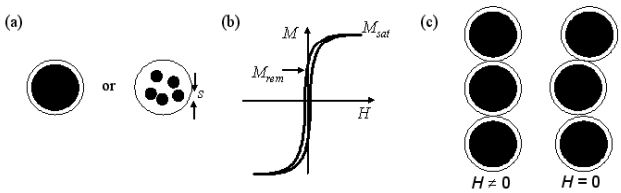

ferromagnetic

M.A.M. Gijs, Microfluid Nanofluid 1, 22 (2004).

9

Protection of the magnetic material

- **Polystyrene coated particles** : uniform size, spherical, hydrophobic surface
- **Magnetic glass particles**: irregular, size distribution
- **Magnetic polysacharide particles**: biocompatible, soft matrix
- **Magnetic poly-(lactic acid) particles**: hydrophobic, biodegradable

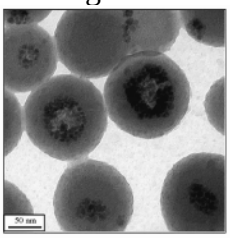

Landfester and Ramirez, J. Phys. Cond. Matter 15, S1345 (2003)

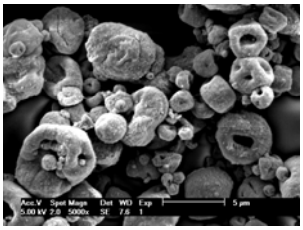

Magnetic Glass Particles, Roche Diagnostics

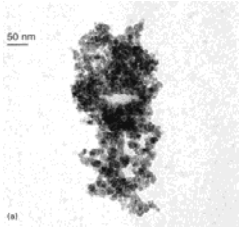

Gruttner and Teller, J. Magn. Magn. Mat. 194, 8 (1999)

10

Chemical functionalization

- Adsorption of proteins to hydrophobic surfaces
- Covalent binding between –COOH, –NH_2, -$CONH_2$, -OH surface groups and NH_2 or –SH groups on the proteins via 'linker' molecules
- Grafting of streptavidin, biotin, histidine, protein A, protein G, etc. on bead surface for specific bio-recognition
- Adsorption of nucleic acids to silica surfaces due to the presence of chaotropic salts in the binding buffer

Magnetostatics

Magnetostatic part of Maxwell's equations

$$\nabla \cdot \mathbf{B} = 0, \qquad (10.1a)$$

$$\nabla \times \mathbf{B} = \mu_0 \mathbf{J}_{\text{tot}} = \mu_0 \mathbf{J}_{\text{ext}} + \mu_0 \mathbf{J}_{\text{mag}}, \qquad (10.1b)$$

where $\mu_0 = 4\pi \times 10^{-7}$ H/m is the magnetic permeability of vacuum, and where $\mathbf{J}_{\text{tot}}$, $\mathbf{J}_{\text{ext}}$ and $\mathbf{J}_{\text{mag}}$ all are stationary current densities; $\mathbf{J}_{\text{tot}}$ the total current density, $\mathbf{J}_{\text{ext}}$ all external transport current densities running in conductors, and $\mathbf{J}_{\text{mag}}$ the current densities bound to magnetic material in the form of atomic/molecular current loops and quantum mechanical spins.

Magnetic dipole moment **m** for a circulating magnetization current I_{mag} enclosing a flat area A

$$\mathbf{m} = I_{\text{mag}} \mathcal{A}\, \mathbf{n}. \qquad (10.2)$$

Magnetization is defined as the magnetic moment density

$$\mathbf{M}(\mathbf{r}_0) = \lim_{\text{Vol}(\Omega^*) \to 0} \left[\frac{1}{\text{Vol}(\Omega^*)^2} \int_{\Omega^*} d\mathbf{r}\, \mathbf{m}(\mathbf{r}_0 + \mathbf{r}) \right]. \qquad (10.3)$$

$$\mathbf{H} = \frac{1}{\mu_0}\mathbf{B} - \mathbf{M}. \qquad (10.5)$$

Using Maxwell equation (10.1a) → $\nabla \cdot \mathbf{H} = -\nabla \cdot \mathbf{M}$

$$\mathbf{J}_{mag} = \nabla \times \mathbf{M}; \qquad (10.4)$$

Inserting (10.4) and (10.5) in Maxwell equation (10.1b) gives

$$\nabla \times \mathbf{H} = \mathbf{J}_{ext}, \qquad (10.6)$$

Definition of magnetic susceptibility

$$\chi \equiv \left(\frac{\partial \mathbf{M}}{\partial \mathbf{H}}\right)_{V,T}. \qquad (10.7)$$

$$\mathbf{M} = \chi\,\mathbf{H}, \qquad (10.8a)$$

$$\mathbf{B} = \mu_0\left(\mathbf{H} + \mathbf{M}\right) = \mu_0\left(1 + \chi\right)\mathbf{H} \equiv \mu_0\mu_r\mathbf{H} \equiv \mu\,\mathbf{H}. \qquad (10.8b)$$

Magnetic bead actuation

- Force in a magnetic field

$$F_x = \mathbf{m} \cdot \frac{\partial \mathbf{B}}{\partial x}$$

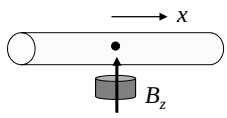

- For superparamagnetic particles in the linear susceptibility regime $(\mathbf{B} = \mu_0\mathbf{H})$, magnetic induction B induces magnetic moment $m = V\Delta\chi\, B/\mu_0$ [Am^2]
  with $V = \frac{4}{3}\pi r^3$ the bead volume,
  $\Delta\chi$ the difference in magnetic susceptibility between the magnetic bead and the surrounding liquid medium,
  B the external magnetic field
- The force becomes $\mathbf{F}_m = \frac{V\Delta\chi}{\mu_0}(\mathbf{B} \cdot \nabla)\mathbf{B}$

- Take bead with r = 0.5 μm and $\Delta\chi$=1 and

  (a) Permanent magnet (∅ = 5 mm)

  B ~ 0.5 Tesla $\Rightarrow$ m= 2×10^{-13} Am^2 and <u>F = 4×10^{-11} N</u>

  (b) Planar coil (∅ = 5 mm)

  B ~ 5 mTesla $\Rightarrow$ m= 2×10^{-15} Am^2 and <u>F = 4×10^{-15} N</u>

- Coils offer flexibility, but magnetic force is very low compared to that of a permanent magnet or magnetized magnetic material

Viscous flow opposes magnetic force

- Viscous drag force on a 1 micron bead

$$F_{x,d} = -6\,\pi\,\eta\,r\,\Delta v_x\,f_D$$

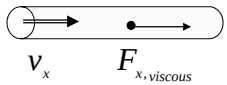

with η = 8.9 x 10^{-4} N s/m^2

and $f_D \approx 1-3$ the drag coefficient.

- Limiting velocity from $m\dfrac{\partial B_z}{\partial x} = -F_{x,d}$
  - Permanent magnet : Δv_x = 4.7 mm/s
  - Coil : Δv_x = 0.47 μm/s
- Coils provide a very low transport speed

Magnetophoretic mobility

- Equalizing magnetic and viscous drag forces:

$$\Delta\mathbf{v} = \frac{2r^2\Delta\chi(\mathbf{B}\cdot\nabla)\mathbf{B}}{9\mu_0\eta f_D} \equiv \frac{1}{\mu_0 f_D}\xi(\mathbf{B}\cdot\nabla)\mathbf{B}$$

with

$$\xi \equiv \frac{2r^2\Delta\chi}{9\eta} = \frac{V\Delta\chi}{6\pi r\eta}$$

the 'magnetophoretic mobility' of the particle,

a parameter describing how magnetically manipulable the particle is

Magnetophoretic mobility of a cell

- Immuno-magnetically labeled cells with different values of antibody binding capacities (ABC), secondary antibody amplification (ψ), or magnetic-particle field interaction parameter ($V\Delta\chi$).
- An increase in any of these parameters will increase the amount of magnetic material bound to the cell and therefore increases the magnetophoretic mobility.

$$\xi_{cell} = \frac{ABC\,\psi\, nV\Delta\chi}{3\pi D_c\eta}$$

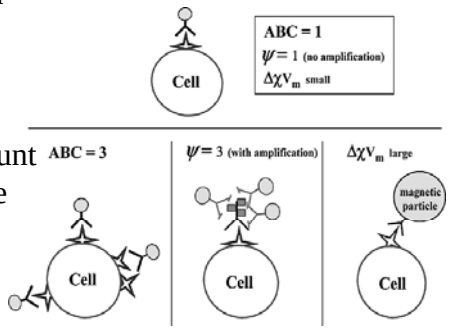

McCloskey, K. E.; Chalmers, J. J.; Zborowski, M. Anal Chem 2003, 75, 6868-6874.

Cell separation methods (i)

- Fluorescence-activated cell sorting (FACS) is done in the flow-through regime and uses laser-induced fluorescence to count and direct droplet-based cells stained with fluorophore-conjugated antibodies against an appropriate CD on the cell surface

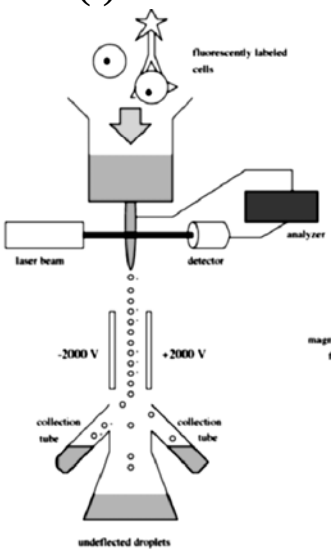

19

Cell separation methods (ii)

- Magnetic cell sorting (MACS) ; cells labeled with superparamagnetic nanoparticles are retained in a high-gradient magnetic field generated by placing a magnetic column in the field of external magnets. Then the column is removed and the retained cells are eluted (positive selection).
- MACS represents only a first sample handling step before additional analysis.

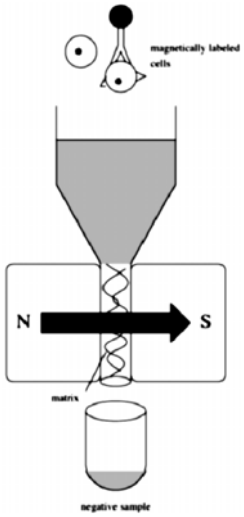

20

Separation systems with macroscopic magnets

Separation: magnetic retention of magnetic beads from a fluid flow

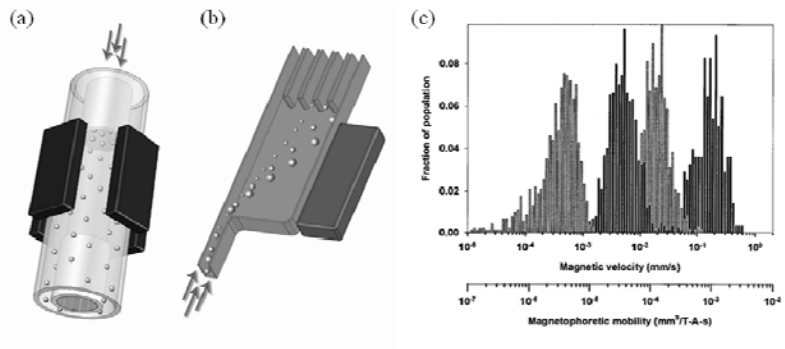

Magnetic quadrupolar and bipolar configurations

M. Nakamura, M. Zborowski, L. C. Lasky, S.Margel, J. Chalmers, J. Experiments in Fluids 30, 371-380 (2001).

21

Magnetic cell separation and purification (i)

- Continuous flow microfluidic device, consisting of magnetic stripes, magnetized by an externally applied field of 0.08 T and placed at a small angle (9.6°) to the direction of the fluid flow.
- Magnetically labeled WBCs are attracted to the stripes and tend to follow the stripe direction, while unlabeled cells do not interact with the stripes and follow the direction of the fluid flow.

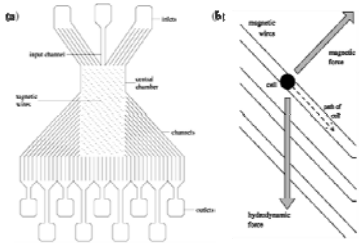

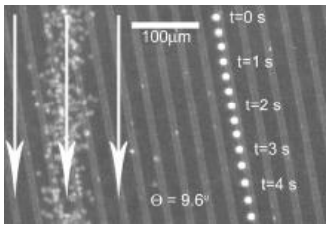

Berger, M.; Castelino, J.; Huang, R.; Shah, M.; Austin, R. H. Electrophoresis 2001, 22, 3883-3892.
Inglis, D. W.; Riehn, R.; Austin, R. H.; Sturm, J. C. Applied Physics Letters 2004, 85, 5093-5095.

22

Magnetic cell separation and purification (ii)

- Separation of *Escherichia coli* cells bound to magnetic nanoparticles in a flow (from left to right) of PBS in a 200 μm wide channel. Images are generated by overlaying sequential frames of movies taken at the beginning, middle and end (left to right) of the microfluidic channel, in the presence or absence of a neodymium disk magnet placed below the channel (bottom and top image, respectively).

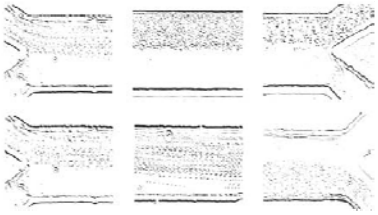

Xia, N.; Hunt, T. P.; Mayers, B. T.; Alsberg, E.; Whitesides, G. M.; Westervelt, R. M.; Ingber, D. E. Biomedical Microdevices 2006, 8, 299-308.

Magnetic cell separation and purification (iii)

Multi-target magnetic activated cell sorter separation architecture

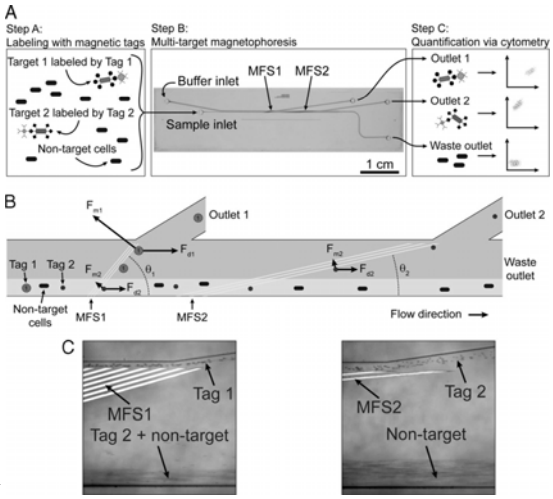

Adams, J. D.; Kim, U.; Soh, H. T. Proceedings of the National Academy of Sciences of the United States of America 2008, 105, 18165-18170.

Magnetic separation of biomolecules

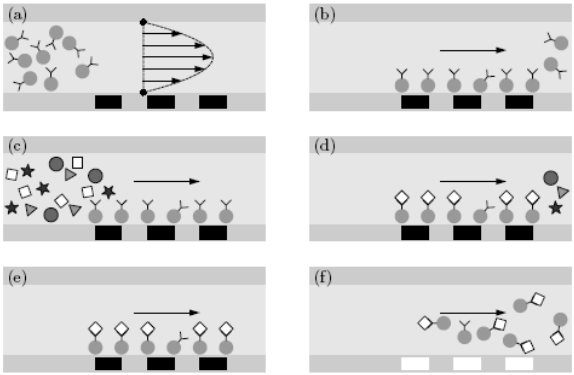

Figure 10.2: The principle in magnetic separation for bio-sampling using magnetic beads flowing in a microfluidic channel. (a) A Poiseuille flow (light gray) carrying magnetic microbeads (dark circles) coated with suitable antibodies (attached Y-shapes). (b) Immobilization of the magnetic antibody-beads by activating magnets (black rectangles) placed in the bottom wall (gray). (c) Introduction of sample containing the target antigen (white squares) and a number of other antigens (triangles, circles and pentagrams). (d) Capture of the target antigen by the immobilized antibody-beads. (e) Thorough rinsing. (f) Release of the target sample by de-activating the magnets (now white rectangles) followed by collection at the microchannel outlet to the right.

Immunoassay by geometrical trapping of magnetic nanoparticle chains

(a) Process flow of the fabrication of the microfluidic chip using dry etching of Pyrex wafer.

(b) SEM picture of the microchannel showing the periodically varying channel width.

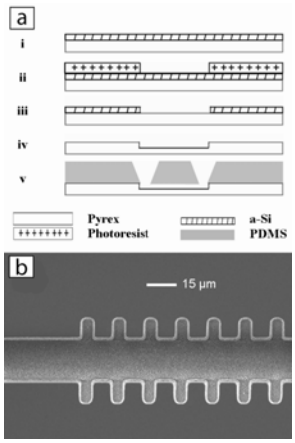

Lacharme, F.; Vandevyver, C.; Gijs, M. A. M., Analytical Chemistry 2008, 80, 2905-2910.

ÉCOLE POLYTECHNIQUE
FÉDÉRALE DE LAUSANNE

(c) Magnetic dipolar energy E_{chain} of a chain consisting of 80 nanoparticles as a function of the displacement *X*.

(d) Magnetic retention force F_{mag} of a chain consisting of 80 nanoparticles as a function of *X*.

(e) Total force on a magnetic chain as a function of liquid flow velocity.

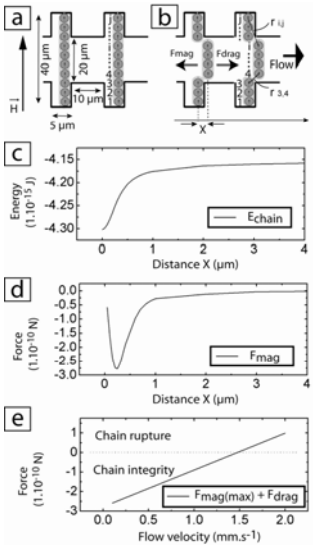

ÉCOLE POLYTECHNIQUE
FÉDÉRALE DE LAUSANNE

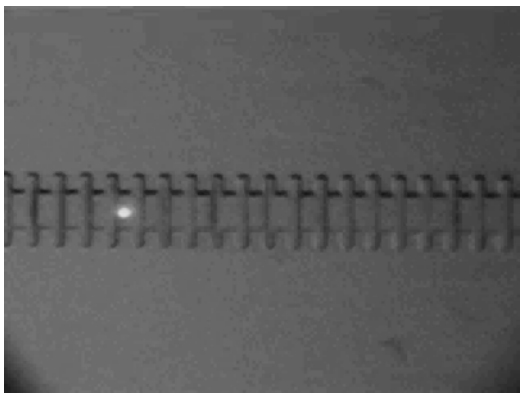

(a) Immunoassay principle. Starting from streptavidin-coated magnetic nanoparticles, biotinylated capture Ab (i), either 5C8 or 5D10 mAb (ii) and fluorescent mouse detection Ab (iii) are subsequently flown through the microchannel.

(b) Fluorescent microscopic image of magnetic nanoparticle chains after the immunoassay.

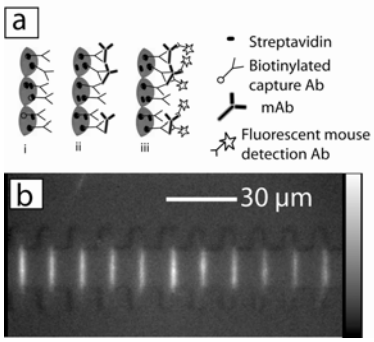

29

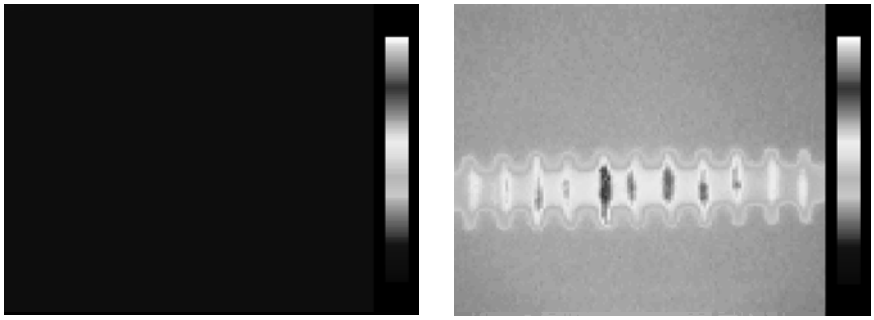

Detection of murine monoclonal antibodies in a non-competitive sandwich immunoassay with a detection limit of 1 $ng.mL^{-1}$ in nanoliters of hybridoma cell culture medium.

30

ÉCOLE POLYTECHNIQUE
FÉDÉRALE DE LAUSANNE

Nanofluidics

Theoretical microfluidics (MICRO-714) – M. Gijs, Th. Lehnert

ÉCOLE POLYTECHNIQUE
FÉDÉRALE DE LAUSANNE

Contents

- Debye layer near charged surface
- Nanofluidic diode
- Nanofluidic protein preconcentrator
- Sea water desalinization
- Direct methanol fuel cell

Debye layer near charged surface

Infinitely away from a charged surface, the two ionic concentrations have the same value c_0 .

Potential at the surface: ζ - potenial .

$$c_\pm(\infty) = c_0, \qquad \phi(\infty) = 0, \qquad \phi(\text{surf}) = \zeta.$$

$$c_\pm(\mathbf{r}) = c_0 \exp\left[\mp \frac{Ze}{k_\mathrm{B}T}\phi(\mathbf{r})\right]$$

Solution for the charge density

$$\rho_\mathrm{el}(\mathbf{r}) = Ze\left[c_+(\mathbf{r}) - c_-(\mathbf{r})\right] = -2Zec_0 \sinh\left[\frac{Ze}{k_\mathrm{B}T}\phi(\mathbf{r})\right]$$

leading to the Poisson-Boltzmann equation

$$\nabla^2\phi(\mathbf{r}) = 2\frac{Zec_0}{\epsilon} \sinh\left[\frac{Ze}{k_\mathrm{B}T}\phi(\mathbf{r})\right]$$

Analytical solution for an infinite planar surface, the Gouy-Chapman solution :

$$\phi(z) = \frac{4k_\mathrm{B}T}{Ze} \operatorname{arctanh}\left[\tanh\left(\frac{Ze\zeta}{4k_\mathrm{B}T}\right) \exp\left(-\frac{z}{\lambda_D}\right)\right]$$

with the Debye length:

$$\lambda_D \equiv \sqrt{\frac{\epsilon k_\mathrm{B}T}{2(Ze)^2 c_0}}$$

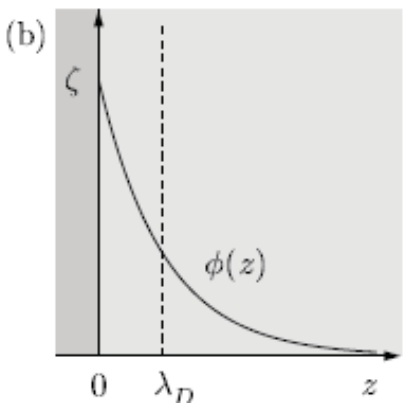

For c_0 = 1 mM = 1 mol/m^3, ε = 78ε$_0$

$$\lambda_D \approx 9.5 \text{ nm}.$$

Debye-Hückel approximation

Debye-Hückel limit : $Ze\zeta \ll k_B T$ → $\sinh(u) \approx u$

$$\nabla^2 \phi(\mathbf{r}) = 2\frac{(Ze)^2 c_0}{\epsilon k_B T}\,\phi(\mathbf{r}) \equiv \frac{1}{\lambda_D^2}\,\phi(\mathbf{r}), \qquad (7.28)$$

For an **infinite planar surface**:

$$\partial_z^2 \phi(z) = \frac{1}{\lambda_D^2}\,\phi(z), \qquad (7.29)$$

Solution:

$$\phi(z) = \zeta\,\exp\left[-\frac{z}{\lambda_D}\right] \quad (z > 0, \text{ single plate wall})$$

Solution of the Poisson equation (7.3b):

$$\rho_{el}(z) = -\epsilon\partial_z^2\phi(z) = -\frac{\epsilon\zeta}{\lambda_D^2}\,\exp\left[-\frac{z}{\lambda_D}\right] \quad (z > 0, \text{ single plate wall})$$

Nanofluidic diode

Combination of nanofluidic channnels with different surface charge can act as a pn diode

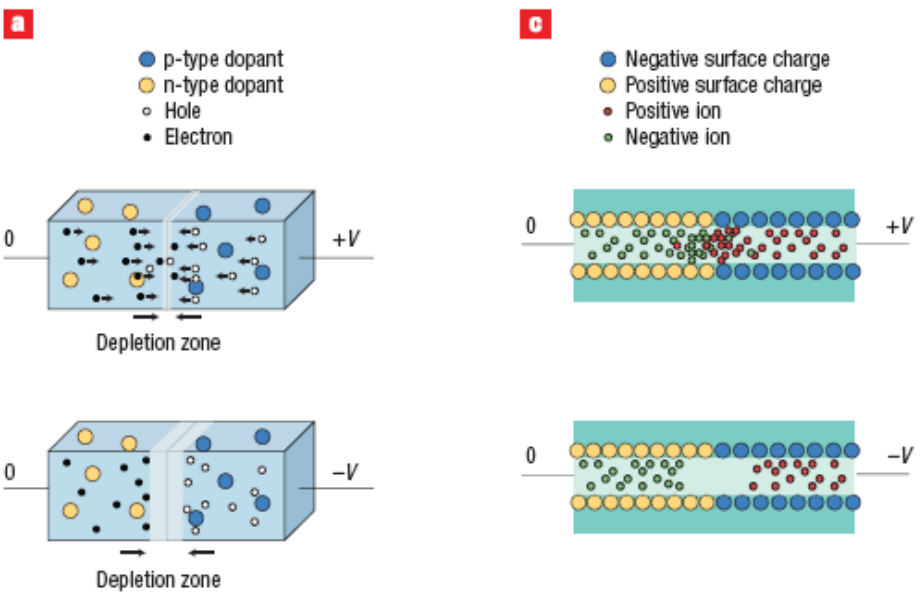

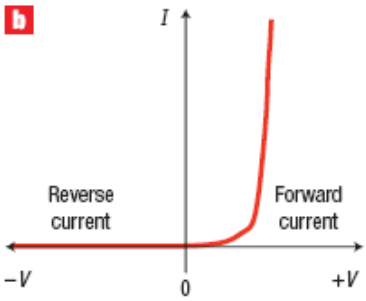

M.A.M. Gijs, Nature Nanotechnology 2, 268-270 (2007).

Conical nanopore

- Nanopore etched in 12-µm-thick polymer membrane. The small opening on one side of the membrane was 2.5 nm and the big opening on the opposite side was 500 nm.
- Carboxyl groups on the inner surface of the as-prepared nanopores provided a natural negative surface charge.
- To make the junction, half of the nanopore interior was coated with positively charged amino groups.

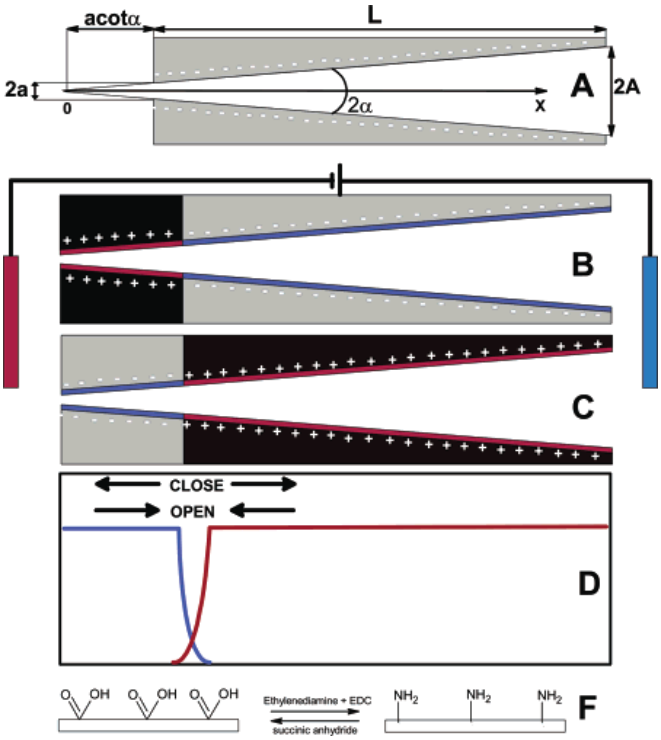

Vlassiouk, I. & Siwy, Z. S. Nano Lett. **7,** 552-556 (2007).

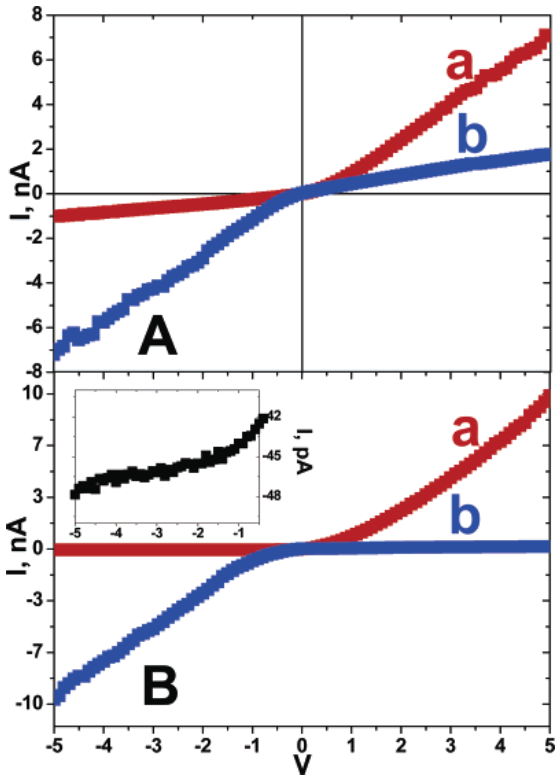

(A) Current-voltage curves for a nanopore modified with amines (a), rendering the surface positively charged, and with carboxyls (b), rendering the surface negatively charged.

(B) Current-voltage curves for a nanofluidic diode: curve a corresponds to positive tip and negative base (left inset shows zoomed negative currents); curve b corresponds to inverse modification.

Vlassiouk, I. & Siwy, Z. S. Nano Lett. **7,** 552–556 (2007).

Nanochannels made in silicon wafers

- 120-µm-long and ~30-nm-high nanofluidic channels using standard silicon clean-room technology.
- Use of diffusion-limited patterning, in which the positively charged protein avidin overcoats negatively charged biotin molecules on the nanochannel wall.

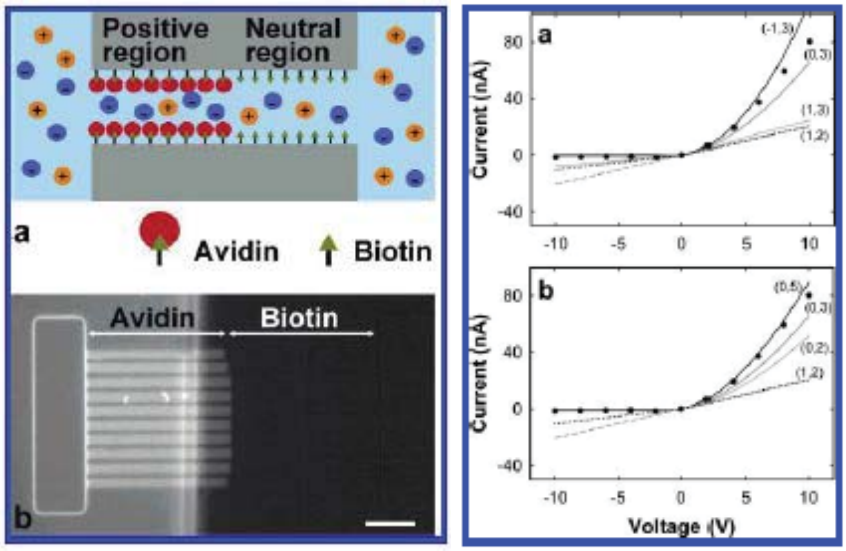

Karnik, R. et al. Nano Lett. 7, 547–551 (2007).

Nanofluidic protein preconcentrator using microchannel-integrated Nafion strip

- Narrow Nafion strip is cut from a commercial Nafion 117 membrane (thickness 175 µm, DuPont). The strip is integrated in a molded PDMS microchannel.
- Nafion has fixed negative charges and a pore mean size of the order of the Electrical Double Layer thickness (1-3 nm).

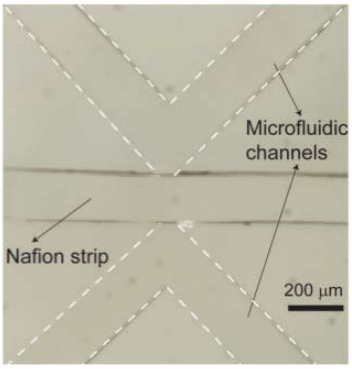

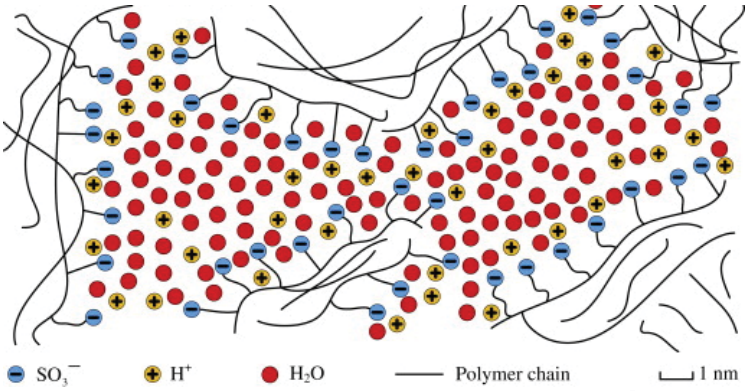

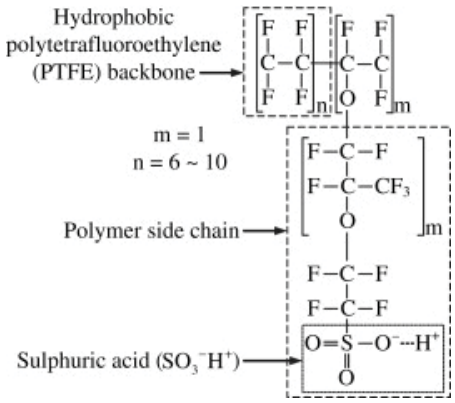

K. Jiao and X. Li, Progr. Energ. Combust Sci. 37, 221-291 (2011).

Operation of the preconcentrator device

- Lower channel is filled with Phosphate Buffered Saline (PBS) (10 mM, pH=7.4) solution.
- Bovine serum albumin (BSA) conjugated with Alexa Fluor® 647 in PBS (60 pM-60 nM) is used as sample solution in the upper channel (pI in water at 25 °C: 4.7).
- Voltages are applied.
- Protein concentration by a factor of 10^4 within a few minutes.

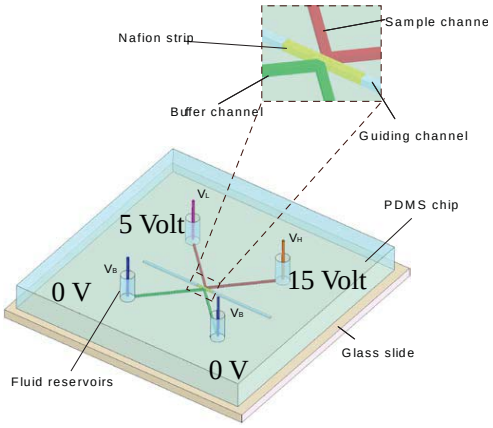

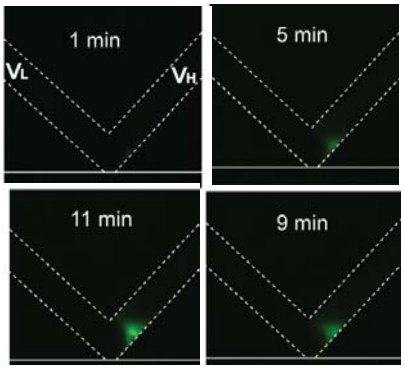

M. Shen, H. Yang, V. Sivagnanam, and M.A.M. Gijs, Analytical Chemistry 82, 9989-9997 (2010).

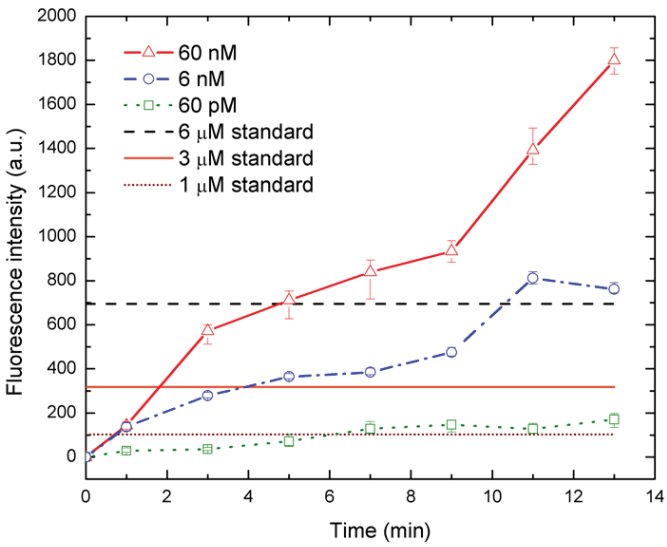

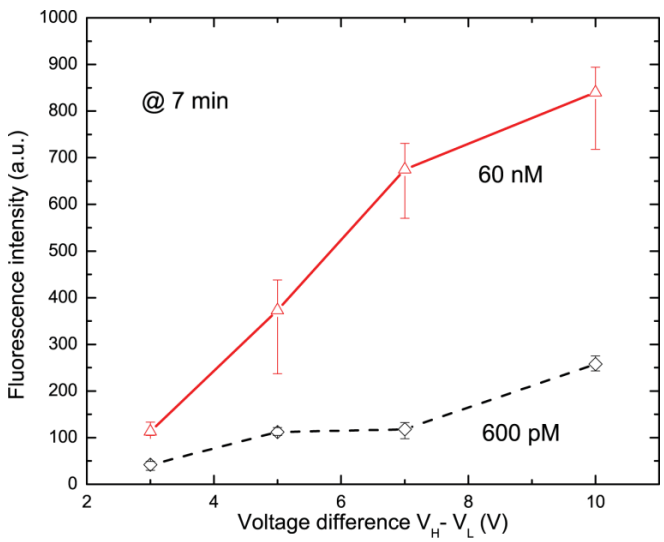

Maximum fluorescence intensity of the preconcentrated plug for AF-BSA concentrations of 60 nM, 6 nM, 60 pM, respectively, with the applied electrical potential difference of 10 V (V_H=15 V, V_L=5 V), and as a function of V_H-V_L.

Numerical model

- Nernst–Planck equation for ionic species transport in fluid medium in the presence of an applied electric field. Positive (i=1), negative (i=2) buffer ions and the tracer molecules (i=3) are considered.

$$\frac{\partial c_i(t)}{\partial t} = \nabla(D_i \nabla c_i(t) + z_i c_i(t) D_i \frac{F}{RT} \nabla \phi(t)) - \nabla c_i(t) \cdot \mathbf{u}(t)$$

- Poisson's equation relates the electric potential and the local concentration distribution of buffer ions and charged tracer molecules

$$\nabla^2 \phi = -\frac{\rho_{fix}}{\varepsilon_0 \varepsilon_r} - \frac{F}{\varepsilon_0 \varepsilon_r} \sum_i z_i c_i(t)$$

Numerical model

- The Navier-Stokes equation and the continuity equation for an incompressible fluid are incorporated into the model.

$$\rho \frac{\partial \mathbf{u}(t)}{\partial t} + \rho(\mathbf{u} \cdot \nabla)\mathbf{u} = -\nabla p + \eta \nabla^2 \mathbf{u} - F \sum_i z_i c_i(t) \nabla \phi$$

$$\nabla \cdot \mathbf{u} = 0$$

- Solving the coupled equations proved to be a highly non-trivial task and a convergent solution was reached if

$$\rho_{fix} / F < (5-10)\,\mathrm{mM}$$

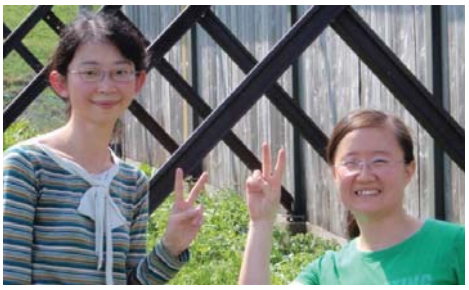

Ion concentration polarization

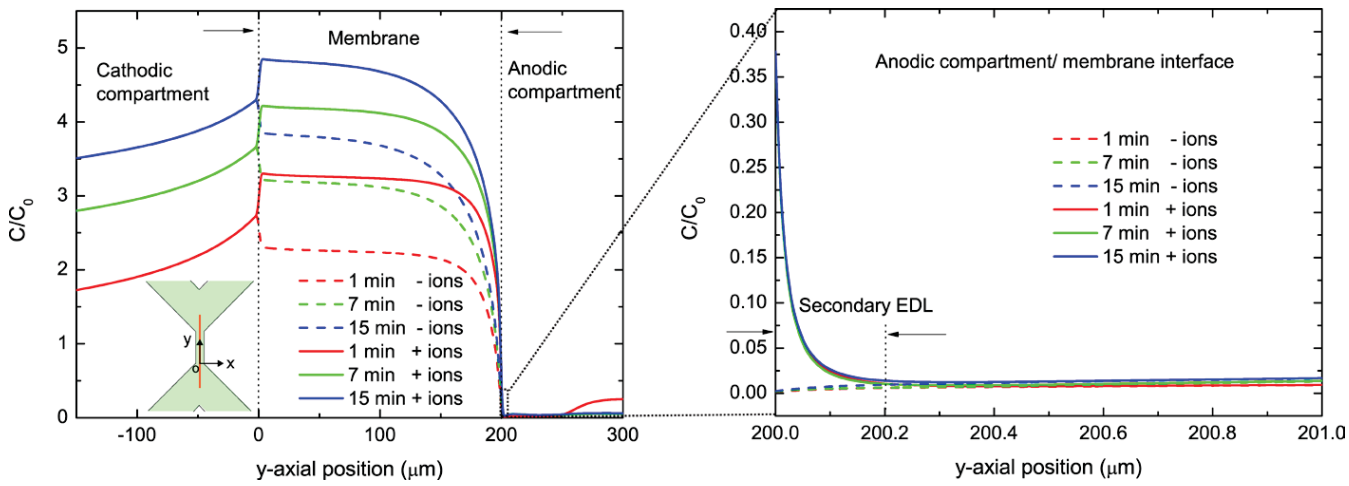

(a) Distributions for positive (full lines) and negative (dashed curves) ions of the background electrolyte after application of the external voltage (V_L=5 V, V_H=15 V) during 1 min, 7 min and 15 min.

(b) Zoom on the ion distributions of the background electrolyte in a region close to the membrane, showing charge imbalance and formation of the Electrical Double Layer.

Microfluidic protein preconcentrator using microchannel-integrated Nafion strip

Numerical study of the preconcentration effect by solving the coupled Poisson, Nernst-Planck and Navier-Stokes equations

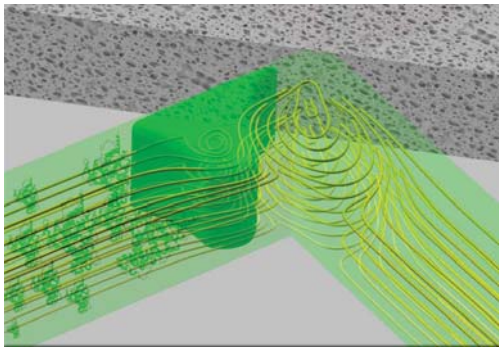

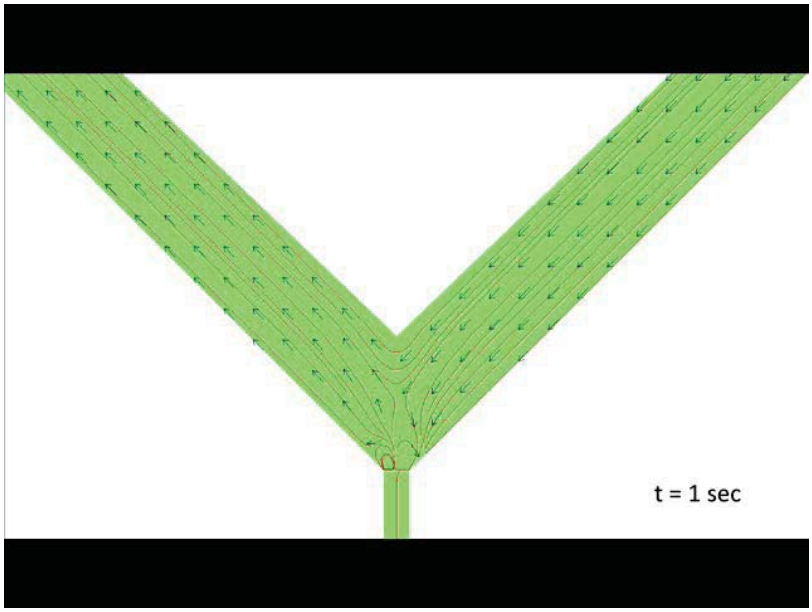

COMSOL Multiphysics™ software

M. Shen, H. Yang, V. Sivagnanam, and M.A.M. Gijs, Analytical Chemistry 82, 9989-9997 (2010).

Seawater desalinisation by Ion Concentration Polarization (IPC)

ÉCOLE POLYTECHNIQUE FÉDÉRALE DE LAUSANNE

- Converting sea water (salinity ~500 mM or ~30 000 mg L^{-1}) to fresh water (salinity <10 mM or <600 mg L^{-1})
- Power consumption of less than 3.5 Wh L^{-1}

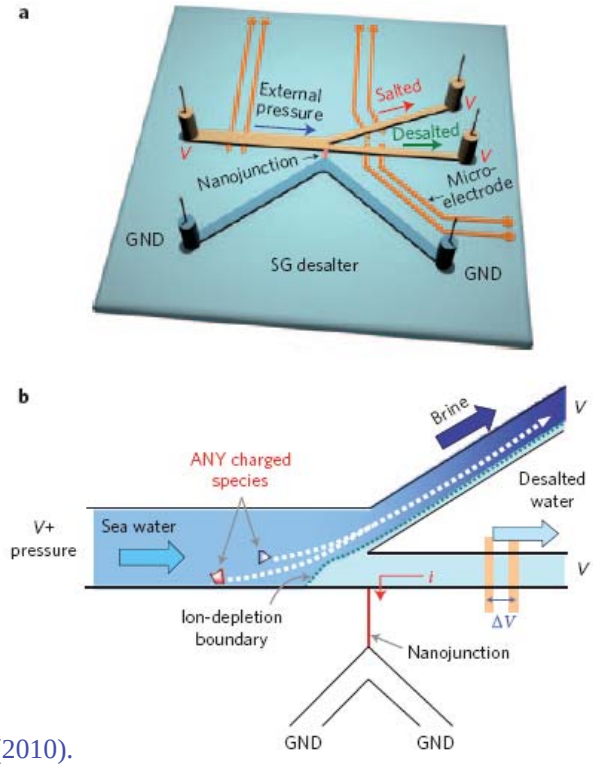

S.J. Kim et al., Nature Nanotechnology 5, 297-301 (2010).

ÉCOLE POLYTECHNIQUE FÉDÉRALE DE LAUSANNE

- a, Fluorescent image tracking of desalination processes with an external flow rate (Q) of 20 ml min^{-1} and applied electric field of 75 Vcm^{-1}. The inlet microchannel has a width of 500 μm and depth of 100 μm.
- b, Fluorescent dyes (representing salts) and WBCs (representing micrometre-sized particles) passed only through the salted stream when ICP was triggered.
- c,d, Microscopic image of each reservoir (salted (c) and desalted (d)) after desalination for 1 h, demonstrating the cleanness of the desalted stream.

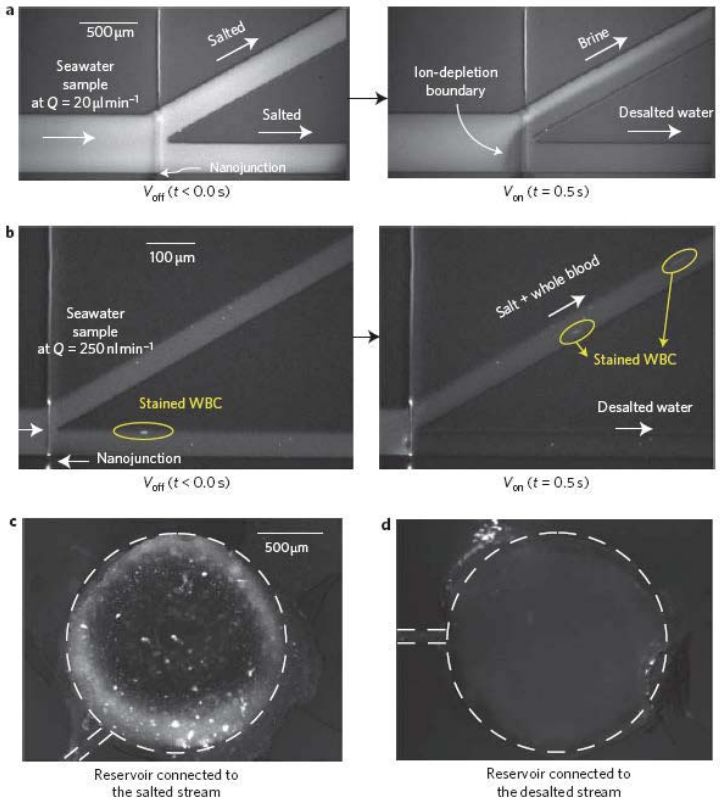

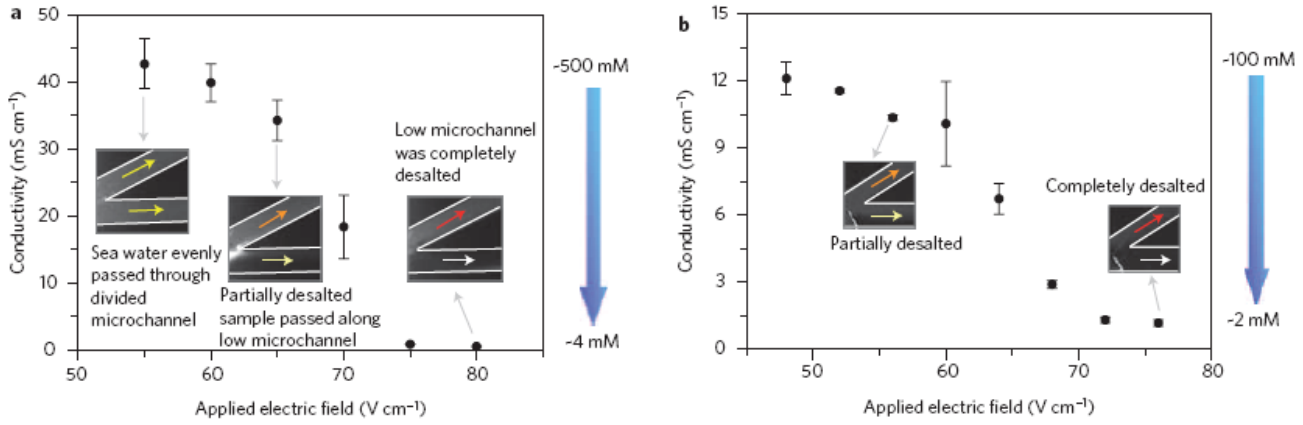

a,b, Conductivity of desalted stream of experiments with a seawater sample (a) and 100 mM phosphate buffer solution (b) as a function of applied electric field. In both cases, the conductivity of the desalted stream dropped to the level of a few mM once the electric field value reached a threshold. This also coincides with the establishment of ICP zones.

Methanol fuel cell using nanoporous Nafion membrane

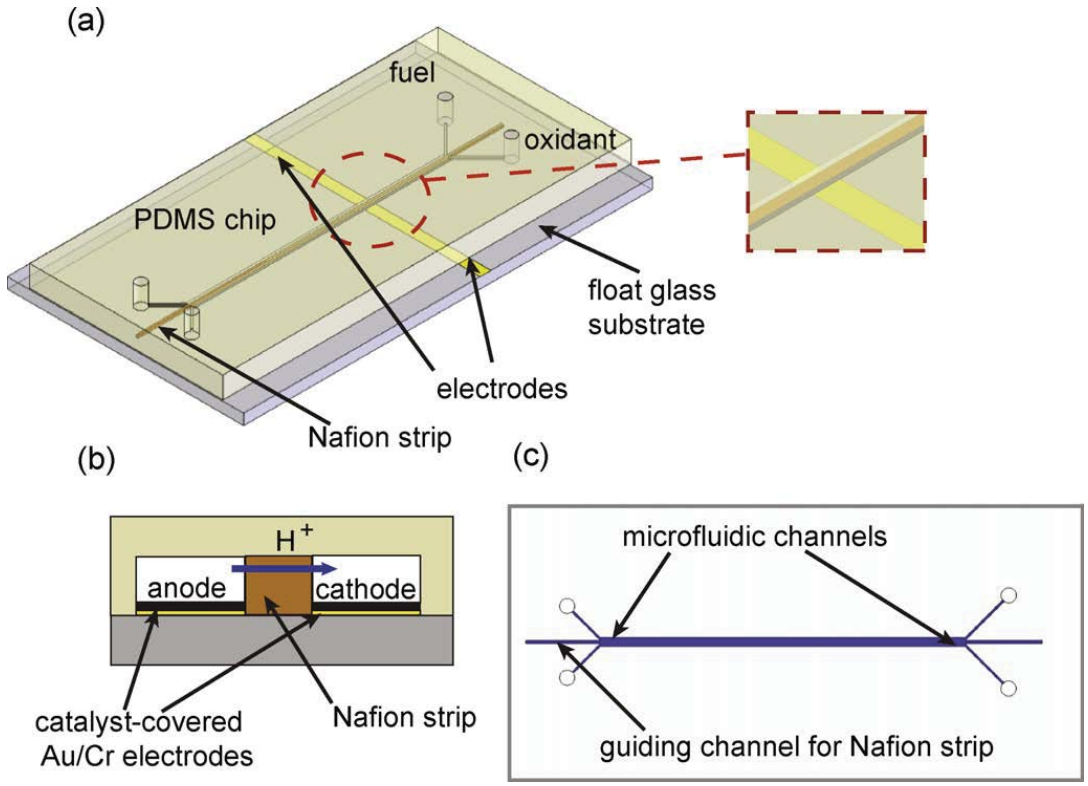

M. Shen, S. Walter, and M.A.M. Gijs, Journal of Power Sources 193, 761-765 (2009).

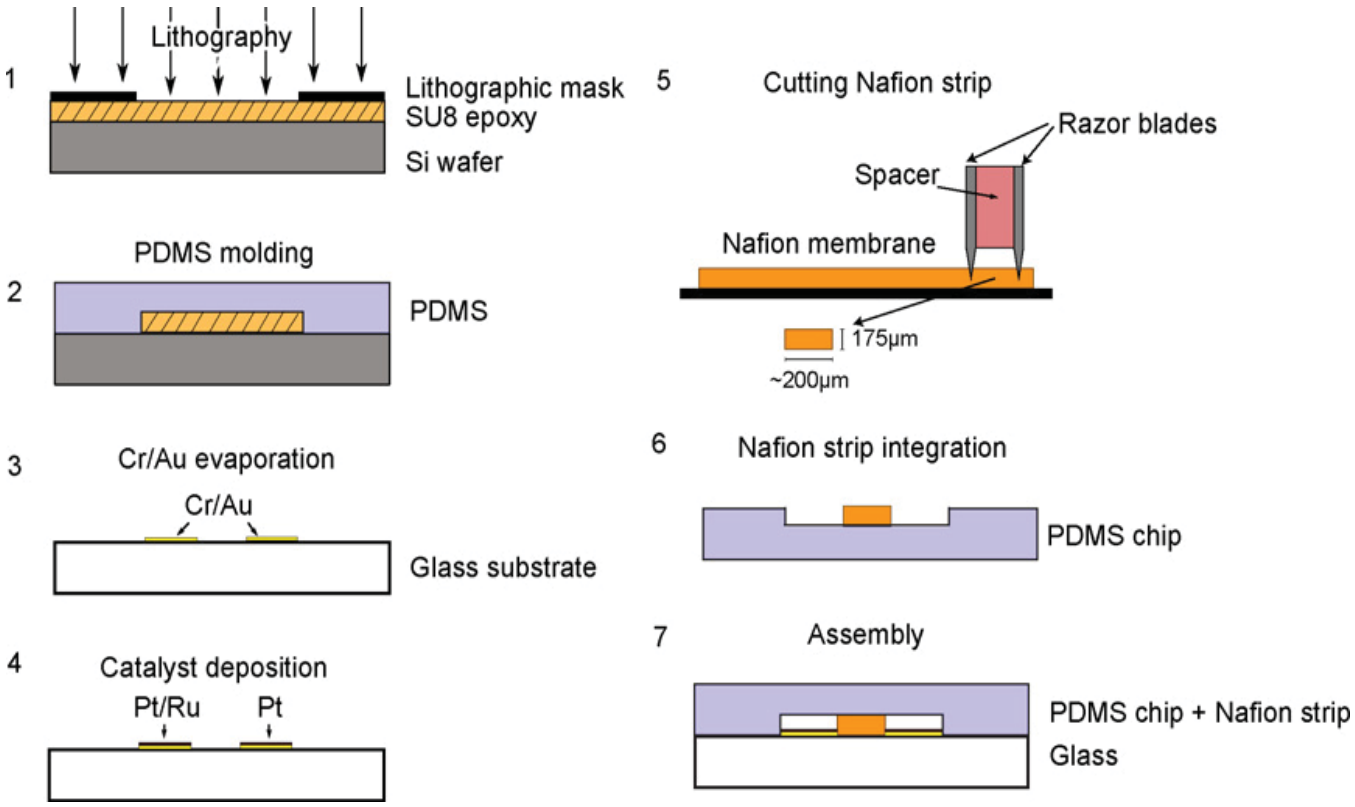

- Fuel (1 M CH_3OH / 0.5 M H_2SO_4) is fed to the anodic microfluidic channel.
- Oxidant
  type I: 0.5 M H_2SO_4 / O_2-saturated
  type II: 0.5 M H_2SO_4 / 0.01 M H_2O_2
  is fed to the cathodic microfluidic channel.

$$\text{Anode}: CH_3OH + H_2O \xrightarrow{Pt/Ru} CO_2 + 6H^+ + 6e^-$$

$$\text{Cathode}: \frac{3}{2}O_2 + 6H^+ + 6e^- \xrightarrow{Pt} 3H_2O$$

$$\text{Overall}: CH_3OH + \frac{3}{2}O_2 \longrightarrow 2H_2O + CO_2$$

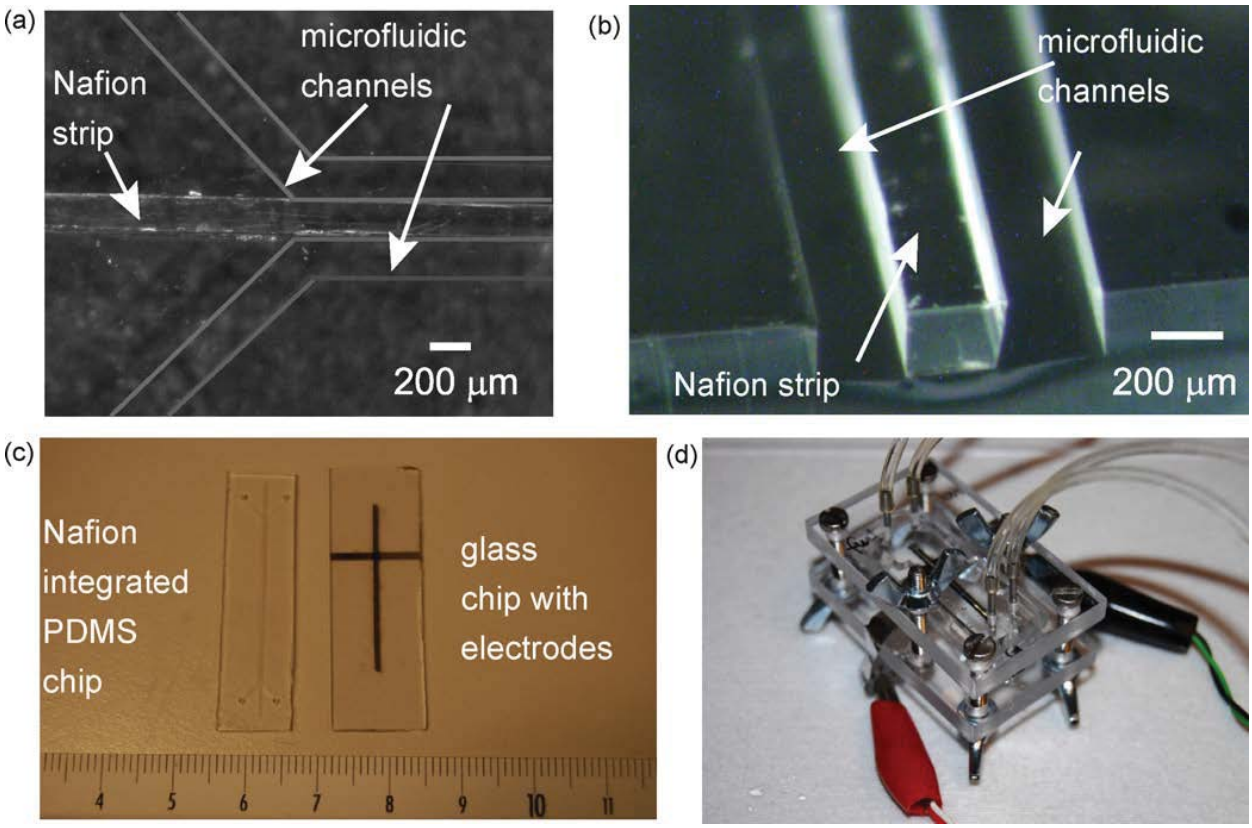

Rapid prototyping of micro-direct methanol fuel cells in PDMS

- Microfluidic channel in PDMS with proton exchange Nafion strip
- Assembly with a glass slide carrying two Au electrodes with Pt-Ru and Pt catalysts
- Stable output voltage of 0.45 V and power up to 3 mW/cm^2

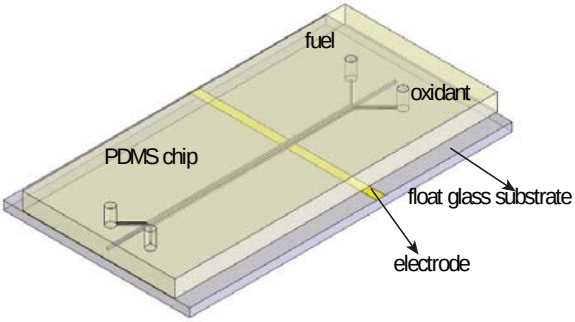

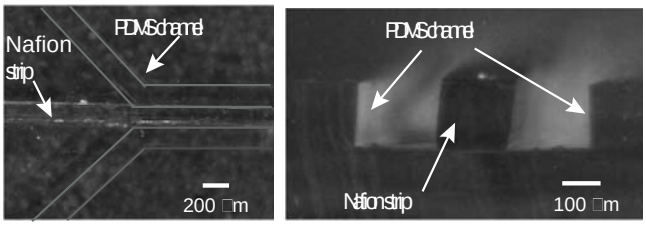

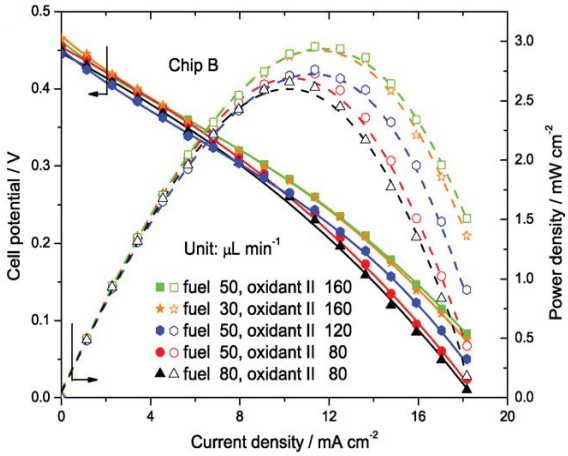

M. Shen, S. Walter, and M.A.M. Gijs, Journal of Power Sources 193, 761-765 (2009).